

## 7<sup>th</sup> MEETING OF THE SCIENTIFIC COMMITTEE

*La Havana, Cuba, 7 to 12 October 2019*

### SC7-SQ14

Correlations between environmental variability and abundance, availability, individual size and body condition of the Humboldt squid (*Dosidicus gigas*).

*Chile*

Correlations between environmental variability and abundance, availability,  
individual size and body condition of the Humboldt squid (*Dosidicus gigas*) in Chile.

Author

Ignacio Payá Contreras

Fisheries Stock Assessment Department  
Chilean Fisheries Development Institute

August 2019

**ABSTRACT**

Jumbo Squid u Humboldt Squid (HS) abundance grew again in Chile in 2002 and it has been one of the main fisheries in this zone since 2011. During the last two years, there have been important changes in this fishery. The objective of this work was to analyze the relationships between environmental variability and abundance, availability, individual size and body condition of HS in Chile. Several regional environmental variables (MEI, NOI, ITCP, ICEN, IOP, HCI), and Chilean oceanographic data (SST, Salinity, Chlorophyll) from fixed stations and scientific surveys were analyzed. HS abundance and/ availability were analyzed based on landings, bycatches and events of squids shore up on beaches. Chilean fisheries were analyze up to July 2019. The historical HS presence in Chile was more frequent in cooling periods. In 2017 the mean landings moved from northern (30-33°S) to southern ports (37°S). In 2019 there were no artisanal landings, and the size and body conditions of squid caught by industry decreased (from 70 to 40 cm ML). October and November Humboldt Current Index (HCI) were correlated with a) landings of the EEZs of Chile, Peru and Ecuador ( $r = 0.70$ ), b) landings of the EEZ of Chile ( $r = 0.68$ ), c) squid size in Perú ( $r=0.60$ ), and d) squid size in Chile ( $r=0.51$ ). While June HCI was correlated with squid body condition in Chile ( $r = 0.69$ ). El Niño 2015-2016 generated a warming that produced waters of lower productivity, which explains the landings displacement from north (30-33°S) to south (37°S) and the activation of the earliest maturation strategy, generating the group of intermediate sizes caught in 2019. The fall squid sizes occurred in Chile two years later than in Peru, probably because the Humboldt current is stronger towards Chilean coasts, attenuating the effect of El Niño, and prolong for longer the high levels of productivity that allow the development of large squids.

## Contenido

I. INTRODUCTION .....	1
II. AIM .....	3
III. DATA AND METHODS .....	3
1. Biology, population dynamics and environment. ....	3
2. Abundance and / or availability indices. ....	3
3. Environmental variability at Chilean and regional levels and historical information on the HS presence in Chilean waters.....	4
4. Correlations between environmental variables and landings of HS at national and regional level. ....	6
5. Biological-fishing indicators of the Chilean fishery until July 2019. ....	6
6. Correlations between environmental variables and biological variables (mantle length and body condition) in the EEZs of Peru and Chile. ....	6
7. Environment and HS spatial distribution change in Chile. ....	7
IV. RESULTS AND DISCUSSION.....	7
1. Biology, population dynamic and environment.....	7
2. Abundance and/or availability indices in Chilean in coastal waters. ....	9
3. Environmental variability at Chilean and regional levels and historical HS presence in Chilean waters.....	10
4. Environmental variables and HS landings in Chile and the region.....	10
5. Biological-fishing indices of Chilean fisheries up to July 2019. ....	11
6. Correlations between environmental variables and biological variables (mantle lengths and body condition) in the EEZs of Peru and Chile. ....	12
7. Relation between environmental changes and HS spatial distribution in Chile.....	12
V. CONCLUSIONS .....	15
VI. REFERENCES .....	16
LISTADO DE TABLAS .....	24
LIST OF FIGURES .....	25
TABLES.....	29
FIGURAS .....	32

## I. INTRODUCTION

The Humboldt Squid (*Dosidicus gigas*), hereafter HS; is an endemic squid in the eastern region of the Pacific Ocean, distributed vertically between the surface and 1200 m and with a geographical range between 40°N (California, United States) and 47°S (South of Chile). In the region of Equator, its range extends and narrows towards the West, reaching 140°W (Nigmatullin *et al.*, 2001). Depending on the environmental conditions, it expands its range to the subtropical areas of both hemispheres (Ehrhardt *et al.*, 1983; Nevárez-Martínez *et al.*, 2006; Ichii *et al.*, 2002; Taipe *et al.*, 2001; Fernández y Vásquez 1995, Field *et al.*, 2007) (Figure 1).

In Chilean waters until 2003, HS presence had been low and with some years of records of large squid washed up on beaches (Wilhem, 1930), and other years with ephemeral squid fisheries of 1-2 years of duration (Schmiede and Acuña 1995; Fernández and Vásquez, 1995; Payá *et al.*, 2004). In that context, when some HS washed up on beaches occurred in 2001, it was thought to be another sporadic event. However, this began a period of high abundance, with HS appearing in the pelagic and demersal fisheries of the central-southern zone (Cubillos *et al.*, 2004), which generated important operational problems in hake fisheries (Payá, 2004). The high HS presence in 2003 led to simulate the effect of HS predation on common hake and recommend applying a precautionary approach in setting hake quotas for 2004 against a possible effect of HS predation (Ehrhardt 1991, Payá *et al.*, 2004; Alarcón-Muñoz *et al.*, 2008). Then possible hake predation by HS and unreported hake catches (under reports and illegal fishing) were incorporated into the hake stock assessment model as an additional mixed mortality, that allowed explaining the great drop in abundance and age structure truncation of common hake (Payá, 2005). This model slightly modified is used until now to do hake stock assessment and management (Tascheri *et al.*, 2018). HS initially considered a plague, which possibly affected other demersal fisheries (Payá *et al.*, 2004; Alarcón-Muñoz *et al.*, 2008), became one of the main artisanal fisheries of the central-south zone (Payá, 2016).

Chilean HS catches have been mainly artisanal and have been made in the regions of Coquimbo (31°S), Valparaíso (33°S) and Talcahuano (37°S) (Payá, 2016). While industrial fleet initially caught HS as bycatch, but since 2011, it has been caught as a targeted species (Payá, 2017). In 2012, the first annual global HS catch quota of 180 thousand tons was established. In 2013, the catch quota rose to 200 thousand tons, and since then it has remained at that value. Since 2014, the quota has been divided, allocating 80% to artisanal fishing and 20% to industrial fishing

(Figure 2). Since August 2019, the Law established “potera” (artisanal jigging) as the only fishing gear allow to fish HS. This new Law in practice inabilities the industrial sector is this fishery.

At the regional level (FAO area 87), HS are caught in the convention area of the South Pacific Regional Fisheries Management Organization, SPRFMO (<https://www.sprfmo.int/>) and in the Exclusive Economic Zones (EEZ) of Chile, Perú and Ecuador (Figure 3). In recent years, HS has become the main species in terms of catches in the SPRFMO area. The whole catch was 724 thousand tons in the FAO area 87 in 2017 (Payá, 2018 a). The Chilean recognizes that the HS is a transzonal resource, therefore, it actively participates in the discussions and work guidelines promoted by the scientific committee of the RFMO-PS, which They mainly include the monitoring of fisheries, the study of connectivity and the identification of the methodology for conducting the stock assessment (Payá, 2018b). There are still no measures to manage the HS in the SPRFMO. Both at the Chilean level and in the SPRFMO, the stock assessment of HS is very complex and it is still in a development stage. In Chile, different methods of stock assessment have been applied, initially assuming the existence of a single Chilean stock, poor data models were applied based catch only and production models (Payá *et al.*, 2014 a and b), but currently it documented the existence of seasonal migration patterns and the development of local depletion events, therefore, intra-annual depletion models have been applied to estimate the biomass that would escape at the end of the year (Payá, 2018 a and b). On the other hand, at the level of the SPRFMO, the existence of a single large stock with the presence of the three morphs is hypothesized, while the stock assessment model is under development (Payá, 2018b).

Until 2016, Chilean artisanal catches were mainly made in the regions of Coquimbo and Valparaíso (30-33°S), but in 2017 the availability of HS decreased significantly in these regions and increased in the Talcahuano region (38°S)(Payá, 2019). In 2018, HS was almost absent in bycatches of hake hydroacoustic survey, in which it had been an important component in previous years (Molina and Rojas, 2019). During 2019, HS has disappeared from the coastal areas and artisanal landings are practically null, while industrial fishery has caught its catch quota. The aim of this paper was to analyze the relationships of environmental variables with abundance, availability, and individual sizes and body conditions of HS in Chile. Therefore, biology, ecology and environment was reviewed, and the Chilean biological-fisheries-environmental information was updated up to July 2019.

## II. AIM (An Index Method)

The aim was to analyze the relationships of environmental variability with abundance, availability, individual sizes and body conditions of HS (*Dosidicus gigas*) in Chile. The following specific objectives were defined:

1. To review the biology, population dynamic and fisheries.
2. To review HS abundance and/or availability indices in Chile.
3. To review the information on environmental variability in Chile and in the Southeast Pacific region and the historical records of HS presence in Chilean waters.
4. To analyze the correlations between environmental variables and HS landings in Chilean and in the region.
5. To update up to July 2019 the biological and fishery indices of the Chilean HS fishery, with special emphasis on mantle length and body condition.
6. To analyze the correlations between environmental variables and biological variables (mantle lengths and body condition) in the EEZs of Chile and Perú.
7. To analyze the relationship between environmental changes and the spatial HS distribution in Chile.

## III. DATA AND METHODS.

### 1. Biology, population dynamics and environment.

Both indexed scientific publications and technical reports of IFOP, IMARPE and PRODUCE in Peru were reviewed, as well as documents and data from the SPRFMO ([www.sprfmo.int](http://www.sprfmo.int)).

### 2. Abundance and / or availability indices.

To analyze changes in HS abundance/availability in Chile, the annual relative abundance indices based on the CPUE (ton/fishing-trip) of small boats ( $\leq 8$  m of total length) with “potera” and large size boats ( $8 \text{ m} < \text{total length} < 20 \text{ m}$ ) with “potera” were used, which were estimate using CPUE standardization models (Payá, 2019). The CPUA index (catch per unit of standard area) from Hydroacoustic hake surveys were also analyzed, where HS is bycatch in the trawl hauls.

To analyze abundance changes at the regional level, landings in the EEZs of Chile, Perú and Ecuador, and in international waters (IW) were compiled from the statistics of the SPRFMO and PRODUCE. For this analysis it was assumed that landings reflect abundance. This assumption is based on the fact that catch quotas are greater than landings in Perú and Chile, and in the absence of any HS management measure in the SPRFMO.

### 3. Environmental variability at Chilean and regional levels and historical information on the HS presence in Chilean waters.

The following regional environmental indices were reviewed:

- a) MEI, which is determined as the first major component of six different parameters: pressure at sea level, zonal and southern surface wind components, sea surface temperature, surface air temperature and cloudiness using data from the International Comprehensive Ocean Atmosphere Data-Set (ICOADS) (Wolter, 1987). The MEI is calculated twelve times a year for each "bi-monthly mobile season." Large positive MEI values indicate the occurrence of El Niño conditions, while large negative MEI values indicate the occurrence of La Niña conditions. The MEI.ext (<https://www.esrl.noaa.gov/psd/enso/mei.ext/rank.ext.html>) was used for 1871-1979 and for 1980-2019 the MEI.v2 ([www.esrl.noaa.gov/psd/enso/mei/](http://www.esrl.noaa.gov/psd/enso/mei/)). To facilitate visualization of long-term variability, the accumulated MEI was calculated and a model with periods of linear growth and decay was fitted. The model was programmed and fitted in R (R Development Core Team, 2009), minimizing the sum of quadratic residuals using the "nlm" function. The model describes the accumulated MEI (MEIA) per year  $i$  ( $i = 1, 2, \dots, N$ ), for different periods  $j$  ( $j = 1, 2, \dots, M$ ), by annual rates for periods:

$$MEIA_i = Rate_j + MEIA_{i-1}$$

where  $MEIA_{i=1}$  and Rate are parameters to be estimated.

- b) The NOI (El Niño Oceanic Index) is calculated as the 3-month moving average of ERSST.v5 SST anomalies in the Niño 3.4 region ( $5^\circ \text{ N}$ - $5^\circ \text{ S}$ ,  $120^\circ$  - $170^\circ \text{ W}$ ) ([https://origin.cpc.ncep.noaa.gov/products/analysis\\_monitoring/ensostuff/ONI\\_v5.php](https://origin.cpc.ncep.noaa.gov/products/analysis_monitoring/ensostuff/ONI_v5.php)).
- c) ICEN (El Niño Coastal Index) was established by the Multisectoral Commission responsible for the Study of the El Niño Phenomenon (ENFEN) for the diagnosis of El Niño and La Niña in Peru (ENFEN, 2012). It is calculated as the three-month moving average of the anomaly of the sea surface temperature in the Niño 1 + 2 region ( $90^\circ$  -



80° W, 10 ° S-0 °) of the ERSST v3b rt product with respect to the weather for the period from 1981-2010.

([http://www.imarpe.pe/imarpe/index.php?id\\_seccion=I0178090300000000000000](http://www.imarpe.pe/imarpe/index.php?id_seccion=I0178090300000000000000)).

- d) ITCP (Peruvian Coastal Thermal Index) is an indicator of the effect of El Niño-Southern Oscillation (ENSO) and of the marine circulation in the thermal variability of the coastal ocean of Peru characterized by the coastal outcrop. It is estimated using the monthly averages of the sea surface temperature obtained from the NOAA NCDC OISST v2 product for the period 1982-2014 (Reynolds *et al.*, 2007). The authors consider the “maximum outcrops area limit” to be the maximum zonal gradient of the annual average sea surface temperature, which determines the thermal front between coastal and oceanic waters. The ITCP is calculated as the three-month moving average of the first principal component (CP1) reduced from thermal anomalies in the coastal zone. The ITCP is expressed in standard deviation units of the CP1 (Quispe-Ccalluari *et al.*, 2016) ([http://www.imarpe.pe/imarpe/index.php?id\\_seccion=I0178090200000000000000](http://www.imarpe.pe/imarpe/index.php?id_seccion=I0178090200000000000000)).

- e) IOP (Peru Oscillation Index) is generated from the SST of 9 coastal stations near IMARPE laboratories. It corresponds to the first main component of the 9 series of monthly anomalies with respect to the average January 1950 to December 2017. The monthly data correspond to the average of the daily data (Purca *et al.*, 2005). This index was extracted from the IMARPE charts (2018).

- f) HCI (Humboldt Current index) is an indicator of the intensity of the ocean-atmosphere process along the Chilean coast. It is calculated using monthly averages of the atmospheric pressure at sea level (SLP) obtained in the weather stations of Antofagasta (23 ° 43'S, 070 ° 45'W) and Easter Island (27 ° 9'S, 109 ° 25'W) (Blanco 2004)(<http://www.bluewater.cl/HCI/>)

Historical HS presence in Chile was inferred from historical records of stranddlings in beaches obtained from the descriptions of Wilhem (1930 and 1951), Fernández and Vásquez (1995) and Cubillos *et al.*, (2007), as well as official statistics of landings.

#### 4. Correlations between environmental variables and landings of HS at national and regional level.

Correlations between annual landings in EEZ (Chilean and regional figures) and HCI by month were estimated. HS variables were typified or normalized, subtracting the average and dividing by the standard deviation. Pearson's linear correlations and their levels of significance were calculated using the "stats" package of R (R Development Core Team, 2009).

#### 5. Biological-fishing indicators of the Chilean fishery until July 2019.

Biological-fishery databases from Chilean fisheries were updated to July 2019. The sampling is routinely done by IFOP scientific observers onboard artisanal boats, and industrial vessels, as well as in the landing ports. Biological databases included random samples of mantle lengths (ML), and detailed biological samples (ML, weight, sex, maturity, etc.). Fisheries databases include fishing industrial logbooks and official database of landings by vessel and boat (SERNAPESCA). Catches and landings were calculated by fleet, month, region and year. The ML medians per year (until 2019) were calculated for the whole Chilean fisheries. Median ML per year (until 2018) in the bycatches of hydroacoustic surveys were taken from Molina and Rojas (2019), while median ML in Peruvian catches per year (until 2018) were obtained from Argüelles and Tafur (2010) and IMARPE (2018) tables. Length-weight relationship in Chilean catches was analyzed using a hierarchical model, where allometric parameters per year were considered random errors taken from hyper-distributions that have a normal density function. The model was programmed in R language (R Development Core Team 2009), using the TMB package (Kristensen *et al.*, 2016). The body conditions were analyzed estimating by year the weights at 30, 40, 50, 60 and 70 cm of ML.

#### 6. Correlations between environmental variables and biological variables (mantle length and body condition) in the EEZs of Peru and Chile.

Correlations between length of 50% of maturity (L50%M) in Peruvian catches and the Oscillation Index of Peru were calculated. The L50%M data were obtained from Argüelles and Tafur (2010) and IMARPE (2018). The correlations between L50%M in Peruvian catches and HCI by month were calculated. The correlations between ML in Chilean EEZ catches and HCI by month were also calculated. Chilean ML was computed concatenating two series, the first one (1999-2001

and 2004-2009) was composed by median ML of bycatches of hake surveys (Molina and Rojas, 2019), and the second one (2010-2019) by median ML of industrial and artisanal catches (2005 was excluded because was caught by hook lines). In addition, the correlations between body condition (weight at 70 cm ML, calculated using hierarchical model parameters) and HCI by month were analyzed.

## 7. Environment and HS spatial distribution change in Chile.

Hovmöller diagrams of the sea surface temperature anomaly (SSTA) by degree of latitude and year were reviewed for zones 18-26°S, 25-33°S and 32-41°S. Diagrams were done by Adriam Bustamente (DOMA-IFOP). SST data were downloaded from <https://www.ncei.noaa.gov/data/sea-surface-temperature-optimum-interpolation/access/avhrr-only/>. Daily weather images (365) from 1990 to 2018 were done. Average and anomalies were calculated from daily data (excluding February 29).

For the central-south zone (30-40°S), the oceanographic information generated by the hydroacoustic hake surveys during August (Angulo *et al.*, 2017, 2018 and 2019) were also reviewed.

## IV. RESULTS AND DISCUSSION.

### 1. Biology, population dynamic and environment.

There are several reviews of the biology, ecology and fisheries of HS (Nigmatullin *et al.*, 2001; Arkhipkin *et al.*, 2015; Ibáñez *et al.*, 2015; Payá, 2019). HS is characterized by rapid growth, early maturity, with a life cycle that lasts no more than 1 or 2 years approximately (Nesis, 1970 and 1983; Ehrhardt *et al.*, 1982; Argüelles, 1996; Nigmatullin *et al.*, 2001; Keyl *et al.*, 2011). In the southern hemisphere, the HS spawns throughout the year, with a greater incidence between October and January (Nigmatullin *et al.*, 2001; Staaf *et al.*, 2008). In Peru, the breeding zone is coastal and is located in the south, there is a main spawning in spring-summer (October-January) and a secondary spawning in autumn-winter (Arkhipkin *et al.*, 2015). Although in Chile it has been determined that HS spawns (González and Chong 2006) and some paralarvae have been found in waters off the south-central coast (Ibáñez *et al.*, 2015), in the EEZ there are no known areas of spawning concentration, nor have HS been found in the spawning process. Depending on the

size of maturity, three morphs or size groups have been identified: small (13-34 cm in Mantle Length); medium (24-60 cm ML); and large (40-100 cm ML). However, it is not clear if these groups are different species or stocks (Nigmatullin *et al.*, 2001).

HS undergoes great changes in its ranges of geographic distribution, growth and maturation, which according to Keyl *et al.*, (2008) would be connected by a triad of physiological and energetic base (Figure 4). The rationale of these authors is that the HS, being a mobile and fast-growing hunter, has high energy requirements and its food availability must change rapidly, in quantity and quality, when it passes from paralarvae to its final size in a few months. Migratory routes must thus change with the spatio-temporal occurrence of prey items as nutritional requirements vary across the different sizes of the HS. During the extensive horizontal and vertical migrations, the HS passes through different bodies of water that would generate a unique history of temperature and nutrition per individual. Individual temperature and nutritional history would determine the onset of ripening, and this in turn would define the size that individuals can reach, because after the first spawning season they die. Therefore, different groups of HS that have different sizes and maturation sizes would have experienced different environmental conditions with respect to temperature and nutrition and would have migrated through different routes. The strategy of small sizes of maturity would allow the population to survive during warm periods of low food availability, while the strategy of large sizes of maturity would maximize fitness during cold periods with abundance of prey. In this context, these authors propose that the predominance of large squids in the EEZ of Peru from 2000-2007, would be associated with a cold period that was evidenced in the SST anomalies of EL Niño 1 + 2 between 1999 and 2007. On the other hand, small squid would predominate outside the EEZs where warmer bodies of water are kept and food availability is lower. Finally, they propose that the expansion of the HS to areas not previously inhabited by HS, such as the Chilean coast, was due to the change of regime from a warm to a cold condition that followed strong La Niña / El Niño 1996- 1998 and the decrease in competing and prey species resulting from fishing exploitation.

In the Gulf of California, the strong El Niño 1997-1998 and 2009-2010 produced negative effects on landings and notable reduction of individual sizes, however, the recovery of the HS after these El Niño events was very different (Robinson *et al.*, 2015). El Niño 1997-1998 produced a sudden drop in landings (80%), but these recovered after 4 years, because later there were negative anomalies of the MEI and positive anomalies of sustained summer wind speeds that increased the productivity. While El Niño 2009-2010 produced conditions of low pressures, decreasing winds, falling chlorophyll-a and low productivity, which remained until 2016 and generated low

abundance (landings) of squid. Both El Niño events generated strong falls (15-30 cm) of individual sizes, triggered by a large reduction in the size of first maturity, the duration of life of individuals, and individual fertility. After El Niño 1997-1998 the sizes recovered after two years, but after El Niño 2009-2010, five years later the sizes had not been recovered.

In Chile, there have been two cohorts that enter the coastal areas, one of the squids born in autumn-winter and the other of summer spawning (Chong *et al.*, 2005; Zúñiga *et al.*, 2008; Ibáñez and Cubillos, 2007). However, Payá (2014), based on modeling of the migratory cycle (Figure 5) and the growth through the modal progression of the size structures (Figure 6), determines that large squid enter coastal areas in November where they remain until October of the following year. This implies that to understand the dynamic of large squid from Chilean coastal areas, it is important to analyze environmental variability in October and November.

## 2. Abundance and/or availability indices in Chilean in coastal waters.

The hydroacoustic hake survey did not register HS presence in 1993 and 1995, but since 2001 the growth of HS relative abundance (CPUA) began, which reached its peak in 2004 (there was no survey in 2003), then declined sharply and kept fluctuating at similar levels from 2006 to 2017, in 2018 there was no HS presence (Figure 7). The CPUE index of small boats with “poteras” also remained at stable levels between 2007 and 2017, while the CPUE of large boats with “poteras” showed a decreasing trend. Although these indices have not yet been updated, they will practically fall to zero in 2019, since, the artisanal landing has been almost zero in this last year (Figure 8).

Chilean HS landings were maximum in 2005, with about 250 thousand tons, then they kept fluctuating around 150 thousand tons, to fall in 2019 to about 30 tons, due to the lack of artisanal catches (Figure 8). Initially the landings were made mainly by artisanal boats, then from 2010 to 2018 mostly by boats and in smaller quantities by industrial ships (because they were assigned 20% of the catch quota) and in 2019 only by the fleet industrial, because the HS has not been available in the coastal zone for artisanal fishing.

At the regional level (FAO Area 87) landings records are available until 2017. Landings appeared in 1992-1995, then disappeared and returned in 2000, beginning a period of sustained but variable growth, in which landings in the EEZs remained relatively stable in 2005-2017, while those of international waters increased in 2011-2017 (Figure 9). The landings of the EEZ have been mainly composed of large size squid (ML > 50 cm) and in international waters for medium sized squid (ML < 60 cm) (Liu *et al.*, 2010; Li *et al.*, 2016).

### 3. Environmental variability at Chilean and regional levels and historical HS presence in Chilean waters.

MEI.ext, MEI and MEI.v2 indices were consistent with each other (Figure 10), which allowed the MEI.ext and MEI.v2 series to be brought together and highlighted the HS presence in the years 1830, 1895, 1907, 1916, 1928-1930, 1940, 1964-1965, 1992-1994 and from 2001 onwards (Figure 11). The accumulated MEI series showed three cooling periods (1987-1924; 1943-1976; 2000-2015) and three heating periods (1925-1942; 1978-1998; 2015-2019) (Figure 12 and Table 1). The persistent HS presence in the last period is verified in the last sustained period of cooling, which was interrupted by El Niño 2015-2016, which seems to start a good warming trend. Before 2000, the HS presence was observed at the beginning, during and at the end of cooling periods, except for the years 1928-1930, 1940 and 1992-1994, which occurred during warm-up periods.

The MEI and NOI were very similar between them and practically the same in terms of their deviations during the years with HS presence, which were characterized by having a high alternation between positive and negative deviations (Figure 13).

The two coastal indices (ICEN and ITCP) of Peru were very similar, and during the years with the HS presence the anomalies were low to medium magnitude and with a high alternation between positive and negative anomalies (Figure 14). On the other hand, HCI of the coast of Chile presented a very different variation from the other indices, showing three clear periods (before 1977, 1978-1997 and 1998-2019), which coincides with the periods evidenced by the accumulated MEI. HS presence in Chile from 2001 onwards coincides with the last period of positive HCI anomalies, although the HS presence between 1993-1994 was verified in an opposite period of negative HCI anomalies.

### 4. Environmental variables and HS landings in Chile and the region.

The highest correlations between HCI and the annual landings in all EEZs were found in October ( $r = 0.7$ ) and November ( $r = 0.68$ ) (Figure 15 and Table 2). Similarly, the highest correlation of HCI and the landings in the Chilean EEZ were obtained for October ( $r = 0.68$ ) (Figure 16 and Table 2).

## 5. Biological-fishing indices of Chilean fisheries up to July 2019.

Chilean artisanal landings of small boats were made mainly in regions 4 (30°S) and 5 (33°S) until 2016. Landings were done throughout all months, but with more intensity in the middle of each year. In 2017 and 2018, the landings were mostly made in the region 8 (37°S), and lasted until July (Figure 17). Similarly, large boat landings were more important in region 5 at the beginning and in region 8 towards the most recent years, and with a seasonality similar to that of small boats, and no records after July in 2017 and 2018 (Figure 18). Both small and large boats have practically made no significant landings in 2019. Therefore, from the artisanal activity it is clear that since 2017 there was a shift in the HS availability from regions 4-5 (30-33°S) to region 8 (37°S). On the other hand, the industrial trawling fleet has historically caught HS in region 8 and during 2019 fished in the same fishing areas, which are located on the edge of the continental shelf, about 50 km from Talcahuano (Figure 19). Since 2016, industrial catches are determined by monthly catch quotas that last until August. During 2019, the industrial fleet waited until May for large squids, and then it started to fish on medium size squids.

During the current period of high HS abundance (2002-2018), both artisanal and industrial fleets have caught large squids (70-80 cm of ML). But in 2019 the squid sizes caught decreased significantly in the industrial catches (median ML of 42 cm), and in the few artisanal catches as well (Figure 20 A). On the other hand, the HS sizes were medium (37-40 cm of ML) in the hake bycatches during hydroacoustic hake surveys in 1999 and 2000, years of very low HS presence in hake surveys, while HS sizes were large (70-80 cm of ML) in 2001-2018, years of high HS abundance. In 2018, although HS presence in the hake survey was almost nothing, 14 squid individuals were caught during the whole survey, the HS were still large (Figure 20 B).

HS sizes (median) in commercial catches were very similar to those obtained in bycatches of hake surveys, and followed the same pattern of change observed in the coasts of Peru, although with a fall in sizes two years later (Figure 21). This two-year delay is probably due to the fact that Humboldt's current is stronger towards the Chilean coasts, which would allow the effect of El Niño to be attenuated, thus prolonging higher productivity levels that allow the development of large HS for longer. The smaller size (55 cm of ML) of catches in Chile in 2005 is not really comparable to the rest of the information, because it was obtained only with hook line fishing. The similarity of the sizes of the commercial catches and of the hake bycatches allowed to approximate a series

of ML for Chile using the data of the cruise until 2009 and then the data of the commercial fishing, this series was used in the later analyzes.

The hierarchical model of the length-to-weight ratio fitted well to the data and allowed describing the variability observed over the years (Figure 22 and Table 3) as a result of the random variability of the allometric parameters (Figure 23 and Table 3), which show that the weights of the largest squids (ML > 60 cm) had a decreasing trend from 2011 to 2018, which intensified in 2019 (Figure 24).

## 6. Correlations between environmental variables and biological variables (mantle lengths and body condition) in the EEZs of Peru and Chile.

The correlation between the IOP and the L50%M of the HS in Peru was high ( $r = 0.7$ ) and statistically significant (Figure 25). The correlation between the monthly HCI and the L50%M of the HS in Peru was significant and maximum in October ( $r = 0.6$ ) (Figures 26 and 27 and Table 2). The correlation between the monthly HCI and the LM in Chile was statistically significant in November ( $r = 0.51$ ) and December ( $r = 0.50$ ) (Figure 28 and Table 2). While the correlation between monthly HCI and body condition (weight at 70 cm ML) in Chile was significant in June ( $r = 0.69$ ) (Figure 29 and Table 2). These correlations are likely to increase when HCI data will be available for the second half of 2019, since from February to July this index fell similarly to the ML and body condition. The correlation of the June HCI with the body condition would be explained because this month delivers an average signal of the productivity that the HS found during the year, while the amount landed and the sizes reached correlates with the condition at the end of the season.

## 7. Relation between environmental changes and HS spatial distribution in Chile

SST Hovmöller diagrams clearly show the impact of warming of El Niño events and post-Niño cold periods from 18 to 41°S (Figure 30 to 32). In the northern zone (18-26°S) there is no HS fishery, but as seen in the HCI analysis, which comes from this area (difference in pressure from Antofagasta and Easter Island), the environmental signals are related both to landing levels (simile of abundance) and to the squid sizes and condition. However, this is not clearly seen with the SST. The period of abundance of HS in central-southern Chile began in 2002 coincidentally with anomalies close to zero, however, during the rest of the period there were hot and cold



events without an apparent relationship with the HS abundance (Figure 30). The variability of the SST anomalies was greater in the coastal zone (0-20 nm) and lower in the oceanic zone (40-200 nm). On the other hand, the cooling during 2018 could have been related to the displacement of the main HS landings from regions 4-5 (30-33°S) to region 8 (37°S). Perhaps, by having the whole information of the year 2019, a more notable change could be observed and related with the fall of HS availability and sizes in the south central area.

In the north-central zone (25-33°S), which includes the artisanal fishing areas Coquimbo (30 ° S) and Valparaíso (33 ° S) ports, the pattern of SST is similar to that of the northern zone, but with more contrast or variability, especially in the propagation of the positive anomalies in the warming of the years 2007 and 2010, and for presenting in the coastal area (0-20 nm) more positive anomalies than in the north zone during the 2000 (Figure 31). In 2017, when the participation of Coquimbo and Valparaíso in the national landings of HS fell, there was a rapid fall of 1°C, anomalies from +0.5 to -0.5, which remained in 2018 (-0.5).

In the central-south zone (32-41°S), which includes the Valparaíso and Talcahuano (36°43'S) fishing zones, the influence of the 2016 warming ends at approximately 37°S, with the start of normal waters ( zero anomalies) to the south, however, in the coastal area (0-20 nm) these waters quickly warmed up the following year (+0.5) (Figure 32). This change in SST seems to be the only event that stands out in 2016-2017 that could be associated with the movement of the squid to the south (inferred from the drop in landings in regions 4-5 and the increase in region 8). This would be explained because the squid would have moved from an area of lower productivity, where the positive anomalies (+0.5) were more persistent, and spatially more homogeneous, towards an area of higher productivity with colder waters due to the upwelling.

The series of SST anomalies for the coastal zone (0-20 nm) and oceanic (40-60 nm) for the north zone (18-26°S) and south-central zone (34-40°S) from 2001 to April 2019 had a similar trend (Figure 33). After 2015 to 2017 warming, there was a cooling to levels similar to those recorded in previous years. During the first 4 months of 2019 the anomalies have been negative in the central-south zone, both coastal and oceanic, while in the north the anomalies have been slightly positive. Chlorophyll at surface concentrations (CLOAS) were higher in the central-south zone (34-40°S) than in the north zone (18-26°S) (Figure 33 d and e). CLOAS concentrations fluctuated seasonally, but remained at the same level in the coastal area (0-20 nm), while in the oceanic area (40-60 nm), seasonal fluctuations were more variable in their magnitudes and presented low

values since 2017, however, these were similar to those recorded in 2007-2009 and in 2012-2014. The decrease in the availability of squid and its sizes could be related to the declining trend registered by CLOAS since 2015 in the ocean area of the south central area, which would make sense if the HS enters from the oceanic area towards seaside.

The profiles by depth and month of the environmental variables between September 2014 and April 2019 (Figures 34 to 40), indicate according to Grendi *et al.* (2019) that "during the month of April the weak El Niño condition was maintained in the equatorial Pacific. Between Arica and Coquimbo the oceanographic conditions were neutral with a moderate warm trend, given the greater coverage of positive thermal anomalies ( $< + 0.5^{\circ}\text{C}$ ) and coastal foci of up to  $+ 1^{\circ}\text{C}$  on the coast of Arica, Iquique, Mejillones and The north of Caldera. From Valparaíso to Corral, temperatures decreased and negative SST anomaly predominated, which were south of Talcahuano  $-1^{\circ}\text{C}$ ".

In general, the environmental variables in the different depth profiles in Arica ( $19^{\circ}\text{S}$ ), Iquique ( $20^{\circ}\text{S}$ ) and Mejillones ( $22^{\circ}\text{S}$ ) had a similar behavior, which shows the impact of El Niño 2015-2017, which generated in 2015-2016 temperatures of  $20-16^{\circ}\text{C}$  in Arica, from  $18-15^{\circ}\text{C}$  in Iquique and Mejillones, and which then decreased by about  $1-2^{\circ}\text{C}$  in 2018-2019 (Figures 34 to 36). Clearly, the intensity of the El Niño event was higher in Arica and decreased to the south. For its part, the concentration of chlorophyll in Arica in the first 20 m depth remained relatively stable within its seasonal fluctuations, while at greater depths it decreased in 2018 and 2019. In Iquique, in general the concentration of Chlorophyll was lower than in Arica and Mejillones, while in Mejillones the levels of chlorophyll and their behavior were more similar to Arica. Consequently, the important environmental changes that occurred in the north zone (Arica to Mejillones) in 2017 coincide with the beginning of the latitudinal changes of HS landings in the central-south zone, and the subsequent fall of HS abundance and sizes in 2019. This is consistent with the high and significant correlations found between the HCl, which is an index generated for the northern zone, and the landings, squid sizes and squid conditions in the central-southern zone.

For the HS fishing area in region 8 ( $37^{\circ}\text{S}$ ), the Coliumo station ( $36^{\circ}32'\text{S}$ ) is available only, since HS fishing in Corral Station ( $40^{\circ}\text{S}$ ) is practically zero. In addition, chlorophyll information is not available. The Coliumo station is coastal (5 nm and 12 nm), however, it shows that the impacts of El Niño 2016-2017 reached up to 40-50m deep and that they are repeated in the summers of 2018 and 2019, with similar intensity, but more superficially (Figure 38 and 39). Also, the springs

of 2017 and 2018 stand out for the emergence of remarkably colder waters at depths greater than 15 m deep that would be related to coastal upwelling events (Bello *et al.*, 2004). This would indicate that in 2017 and 2018 these upwellings could have allowed the arrival of HS to the Talcahuano area. The presence of cold water upwellings intensifies in the Corral area in the spring of 2018 and summer of 2019 (Figure 40).

The oceanographic information generated in the Hydroacoustic hake surveys during July-August through the years in its latitudinal (30-40°S) oceanographic sections of temperature, salinity and dissolved oxygen concentration, shows El Niño 2015 increased temperature, decreased salinity and increased oxygen concentration (Figure 41). In 2016 and 2017 the temperature increased and the salinity deepened, especially north of 35°S. In terms of productivity, a decrease in chlorophyll concentrations was observed between 2016 and 2017, which were lower than the north of 36°S (Figure 42). Therefore, during 2017 the HS experienced a clear north-south oceanographic gradient, which probably determined the displacement towards the south and the greater participation of Talcahuano in the national landings. The displacement of large sizes to more productive areas was also verified in 2017 on the coasts of Peru, where large squids were fished in the northern zone (9°S), and medium-sized squids in the southern area (16-18°S), in response to the productivity changes produced by the coastal El Niño (IMARPE 2018). In 2018, the hake surveys in Chile did not detect HS presence, and it was observed that the highest concentrations of chlorophyll-a were found in the Gulf of Arauco (37°S), just north of Punta Lavapié (Angulo *et al.*, 2019), very close to the industrial fishing area of HS in front of Talcahuano.

## V. CONCLUSIONS

1. Historical HS presence in Chile was more frequent in cooling periods, although some have been recorded during warm-up periods.
2. El Niño 2015-2016 generated a warming that spread to the central-south zone and generated a gradient of environmental conditions that probably displaced the squid from Coquimbo-Valparaíso (30-33°S) to Talcahuano (37°S) in 2017.
3. During the second half of 2018, HS abundance declined markedly, and disappeared from the bycatches in the hake surveys that takes place in August.

4. During 2019, HS was absence in coastal areas where artisanal fishing operates, and therefore, artisanal landings were almost to zero.
5. During 2019, industrial vessels caught its monthly quotas in its traditional fishing ground in Talcahuano area (38°S), obtaining only medium-sized squids, because of disappearance of large-sized squids.
6. HS body condition decreased from 2011 to 2018, and fell sharply in 2019.
7. Because the large-sized squid enters in November to Chilean coasts and leaves them in October of next year, environmental variability in these months is key to understanding its dynamic.
8. October and November Humboldt Current Index (HCI) is correlated with: a) whole landings of EEZs of Chile, Peru and Ecuador ( $r = 0.70$ ); b) with landings of Chilean EEZ ( $r = 0.68$ ); c) squid sizes in Peru ( $r = 0.60$ ); c) squid sizes in Chile ( $r = 0.51$ ). While June HCI correlates with the HS body condition in Chile ( $r = 0.69$ ).
9. El Niño 2015-2016 generated a warming that produced waters of lower productivity, which activated the earliest maturation strategy, generating the group of intermediate sizes that were caught by the industrial fleet in 2019.
10. The changes in HS abundance and the fall in HS sizes in the central-southern zone of Chile are consistent with the changes observed in Peru and the Gulf of California, after El Niño event followed by a period of low productivity.
11. HS sizes fall in Chile occurred two years after in Peru, probably because the Humboldt current is stronger towards the Chilean coast, which would allow to attenuate the impact of El Niño, and thus prolong longer productivity levels that allow the development of large squid.

## VI. REFERENCES

- Alarcón-Muñoz R., L., Cubillos y C. Gatica. 2008. Jumbo squid (*Dosidicus gigas*) biomass off central Chile: effects on Chilean hake (*Merluccius gayi*). CalCOFI Rep. 49, 157-166
- Angulo, J., V. Valenzuela, S. Núñez, S. Vásquez, R. Luna, y J. Saavedra. 2017. Distribución espacial y batimétrica huevos y larvas y condiciones bio-oceanográficas asociadas. En: Evaluación directa de merluza común, año 2016. Convenio de desempeño 2016. Instituto de Fomento Pesquero.

- Angulo, J., F. Osorio, E. Velasco, S. Núñez, S. Vásquez, R. Luna, y J. Saavedra. 2018. Distribución espacial y batimétrica huevos y larvas y condiciones bio-oceanográficas asociadas. En: Evaluación directa de merluza común, año 2017. Convenio de desempeño 2017. Instituto de Fomento Pesquero.
- Angulo, J., F. Osorio, J. Bonicelli, *et al.* 2019. Distribución espacial y batimétrica huevos y larvas y condiciones bio-oceanográficas asociadas. En: Evaluación directa de merluza común, año 2018. Convenio de desempeño 2018. Instituto de Fomento Pesquero.
- Argüelles, J. 1996. Crecimiento y reclutamiento del calamar gigante *Dosidicus gigas* en el Perú (1991 a 1994). Informe Progresivo n° 23. 1–14 pp.
- Argüelles, J. and R. Tafur. 2010. New insights on the biology of the jumbo squid *Dosidicus gigas* in the northern Humboldt Current System: Size at maturity, somatic and reproductive investment. *Fisheries Research* 106:185-192.
- Bello S., Barbieri M.A., S. Salinas, y L. Soto. 2004. Surgencia costera en la zona central de Chile, durante el ciclo El Niño-La Niña 1997-1999. En: Avaria, J. Carrasco, J. Rutllant y E. Yáñez. (eds.). 2004. El Niño-La Niña 1997-2000. Sus Efectos en Chile. CONA, Chile, Valparaíso. pp. 77-94.
- Blanco, J. L. 2004. Inter-Annual to Inter-Decadal Variability of Upwelling and Anchovy Population off Northern Chile. A Dissertation submitted to the Faculty of Old Dominion University as Requirement for the Degree of Doctor of Philosophy in Oceanography. Old Dominion University, December 2004.
- Chong J., C. Oyarzún, R. Galleguillos, E. Tarifeño, R.D. Sepúlveda, y CM. Ibáñez. 2005. Parámetros biológico-pesqueros de la jibia, *Dosidicus gigas* (Orbigny, 1835) (Cephalopoda: Ommastrephidae) frente a la costa de Chile central (29°S y 40°S) durante el período 1993–1994. *Gayana (Concepción)* 69: 319–328.
- Cubillos L., C. Ibáñez, C. González, y A. Sepúlveda. 2004. Pesca de Investigación: Pesca de Jibia (*Dosidicus gigas*) con red de cerco entre la V y X Regiones, año 2003. Instituto de Investigación Pesquera, Talcahuano, 48 p.

- Cubillos L., M. Pedraza, C. Alarcón, H. Arancibia y M. Barros. 2007. Anexo 2. Varazones de Jibia en Chile En FIP 2005-38. Impacto de la jibia en pesquerías chilenas de peces demersales.
- Fernández, F. y J. Vásquez. 1995. La jibia gigante *Dosidicus gigas* (Orbigny, 1835) en Chile: Análisis de una pesquería efímera. Estudios Oceanológicos (Chile). 14:17-21.
- Ehrhardt, N., Jacquemin, P., Solís, A., García, F., González, G., Ortiz, J. y Ulloa, P. 1982. Crecimiento del calamar gigante *Dosidicus gigas* en el Golfo de California, México, durante 1980. Ciencia Pesquera 3, 33–39.
- Ehrhardt, N., P. Jacquemin, F. García, G. Gonzalez, J. López, J. Ortiz, & A. Solís. 1983. On the fishery and biology of the giant squid *Dosidicus gigas* in the Gulf of California, México. FAO Fisheries Technical Paper 231: 306-340.
- Ehrhardt, N. 1991. Potential impact of a seasonal migratory jumbo squid (*Dosidicus gigas*) stock on a Gulf of California sardine (*Sardinops sagax caerulea*) population. Bulletin of Marine Science 49 (1-2): 325-332.
- ENFEN, 2012. Definición operacional de los eventos el niño y la niña y sus magnitudes en la costa del Perú. Comité Técnico del Estudio Nacional del Fenómeno El Niño (ENFEN).
- Fernández, F. y J. Vásquez. 1995. La jibia gigante *Dosidicus gigas* (Orbigny, 1835) en Chile: Análisis de una pesquería efímera. Estudios Oceanológicos (Chile). 14:17-21.
- Field, J., K. Baltz, A. J. Philips & W. A. Walker 2007. Range expansion and trophic interactions of the jumbo squid, *Dosidicus gigas*, in the California Current. CalCOFI Rep., Vol. 48: 131-146.
- González, P. y J. Chong. 2006. Biología reproductiva de *Dosidicus gigas* D'Orbigny 1835 (Cephalopoda, Ommastrephidae) en la zona norte-centro de Chile. Gayana. 70(2): 237-244.

- Grendi, C., A. Bustamante, C. Salinas, y U. Cifuentes. 2019. Oceanografía e información satelital. En Boletín bio-oceanográfico n°8. Convenio de Desempeño 2018. Condiciones bio-oceanográficas y evaluación del stock desovante de anchoveta entre la XV y II regiones, año 2018. SUBSECRETARÍA ECONOMÍA Y EMT. 17 pp.
- Ibáñez, C.M. & L.A. Cubillos. 2007. Seasonal variation in the length structure and reproductive condition of the jumbo squid *Dosidicus gigas* (d'Orbigny, 1835) off central-south Chile. Sci Mar 71:123–128.
- Ibáñez, C. M., L. A. Cubillos, R. Tafur, J. Argüelles. C. Yamashiro, & E. Poulin. 2011. Genetic diversity and demographic history of *Dosidicus gigas* (Cephalopoda: Ommastrephidae) in the Humboldt Current System. Mar. Ecol. Prog. Ser. (43): 163–171.
- Ibáñez, C. M., R.D. Sepúlveda, P. Ulloa, F. Keyl, y C. Pardo-Gandarillas. 2015. The biology and ecology of the jumbo squid *Dosidicus gigas* (Cephalopoda) in Chilean waters: a review. Lat. Am. J. Aquat. Res. 43(3) 402-414.
- Ichii, T., K. Mahapatra, T. Watanabe, A. Yatsu, D. Inagake & Y. Okada. 2002. Occurrence of jumbo flying squid *Dosidicus gigas* aggregations associated with the countercurrent ridge off the Costa Rica Dome during 1997 El Niño and 1999 La Niña. Mar. Ecol. Prog. Ser. 231:151-166.
- IMARPE. 2018. Situación del calamar gigante durante el 2017 y perspectivas de pesca para el 2018. IMARPE 12 pp.
- Keyl F., J. Argüelles, L. Mariátegui, R. Tafur, M. Wolff, & C. Yamashiro. 2008. A hypothesis on range expansion and spatio-temporal shifts in size-at-maturity of jumbo squid (*Dosidicus gigas*) in the eastern Pacific Ocean. CCOFI Rep 49:119–128.
- Keyl F., J. Argüelles, & R. Tafur. 2011. Interannual variability in size structure, age, and growth of jumbo squid (*Dosidicus gigas*) assessed by modal progression analysis. ICES Journal of Marine Science (2011), 68(3), 507–518. doi:10.1093/icesjms/fsq167

- Kristensen, K., A. Nielsen, C. W. Berg, H. Skaug, & B. M. Bell. 2016. TMB: Automatic Differentiation and Laplace Approximation. *Journal of Statistical Software*, 70(5), 1-21. doi:10.18637/jss.v070.i05.
- Li, G., X. Chen, X. Zou, & B. Liu. 2016. China's National Report Part II: Squid Jigging Fishery. National Data Center for Distant-water Fisheries, Shanghai Ocean University. SC-04-11. SPRFMO.
- Liu, B., X. Chen, H. Lu, Y. Chen & W. Qian. 2010. Fishery biology of the jumbo flying squid *Dosidicus gigas* off the Exclusive Economic Zone of Chilean waters. *Sci. Mar.*, 74 (4): 687-695.
- Molina E. y M. Rojas. 2019. Fauna Acompañante en: Evaluación directa de merluza común, año 2018. Convenio de desempeño 2018. Instituto de Fomento Pesquero.
- Nevárez-Martínez, M., F. J. Méndez-Tenorio, C. Cervantes-Valle, J. López-Martínez & M. L. Anguiano-Carrasco. 2006. Growth, mortality, recruitment, and yield of the jumbo squid (*Dosidicus gigas*) off Guaymas, Mexico. *Fisheries Research*. 79: 38-47.
- Nesis, K. N. 1970. The biology of the giant squid of Perú and Chile, *Dosidicus gigas*. In *Oceanology*. Vol 10. n° 1. 108-118 pp.
- Nesis, K.N., 1983. *Dosidicus gigas*. In: Boyle, P.R. (Ed.), *Cephalopod Life Cycles, Species Accounts*, vol. 1. Academic Press, London, pp. 108–118, 475.
- Nigmatullin, C., K. Nesis & A. Arkhipkin. 2001. Review of the biology of the jumbo squid *Dosidicus gigas* (Cephalopoda: Ommastrephidae). *Fisheries Research* 54: 9-19.
- Payá, I. 2005. Investigación CTP merluza común 2005. Fase II. Instituto de Fomento Pesquero. 41 pp + 6 anexos. DOI: 10.13140/RG.2.1.2581.7842.
- Payá, I. 2014. Evaluación de stock, crecimiento y migración. En Payá *et al.*, 2014a. Estatus y posibilidades de explotación biológicamente sustentables de los principales recursos



pesqueros nacionales al año 2015. Jibia. Informe de Estatus y Cuota. Subsecretaría de Economía - IFOP. 83 pp.+ 4 Anexos.

Payá, I. 2015. Estatus y posibilidades de explotación biológicamente sustentables de los principales recursos pesqueros nacionales al año 2016. Jibia. Informe de Estatus y Cuota. Subsecretaría de Economía - IFOP. 85 pp + 4 Anexos. DOI: 10.13140/RG.2.1.1951.3369.

Payá, I. 2016. Estatus y posibilidades de explotación biológicamente sustentables de los principales recursos pesqueros nacionales al año 2016. Jibia. Informe Consolidado. Subsecretaría de Economía - IFOP. 92 pp + 5 Anexos. DOI: 10.13140/RG.2.2.20164.63365.

Payá I, 2017. Estatus y posibilidades de explotación biológicamente sustentables de los principales recursos pesqueros nacionales año 2017. Jibia. Documento consolidado. Subsecretaría de Economía - IFOP. 99 pp + 5 Anexos.

Payá I, 2018a. Estatus y posibilidades de explotación biológicamente sustentables de los principales recursos pesqueros nacionales año 2018. Jibia. Documento consolidado. Subsecretaría de Economía - IFOP. 110 pp + 4 Anexos.

Payá I, 2018b. Depletion models with successive pulses of Humboldt squid (*Dosidicus gigas*) in coastal waters off Central Chile. SC6-SQ05. 21 pp + Annex. <https://www.sprfmo.int/assets/2018-SC6/Meeting-Documents/SC6-SQ05-Depletion-models-with-successive-pulses-of-Humboldt-squid-in-coastal-waters-off-Central-Chile.pdf>

Payá I, 2019. Estatus y posibilidades de explotación biológicamente sustentables de los principales recursos pesqueros nacionales año 2019. Jibia. Documento consolidado. Subsecretaría de Economía - IFOP. 118 pp + 3 Anexos.

Payá I, L. Caballero, A. Barraza, J. Cavieres, A. Yáñez y R. Tascheri. 2014a. Estatus y posibilidades de explotación biológicamente sustentables de los principales recursos

pesqueros nacionales al año 2015. Jibia. Informe de Estatus y Cuota. Subsecretaría de Economía - IFOP. 83 pp.+ 4 Anexos.

Payá, I., R. Tascheri y J. Sateler. 2004. Investigación CTP merluza común 2004. Instituto de Fomento Pesquero. 98.

Payá I, C. Canales, D. Bucare, M. Canales, F. Contreras, F. Espíndola, E. Leal, C. Montenegro, J. Quiroz, R. Tascheri, María J. Zúñiga. 2014b. Revisión de los puntos biológicos de referencia (Rendimiento Máximo Sostenible) en las pesquerías nacionales." Primer Taller internacional. Informe de Avance 1. Subsecretaría de Economía - IFOP. 32 pp.+ 4 Anexos.

PRODUCE. 2012. Anuario estadístico pesquero y acuícola 2011. Ministerio de la Producción del Perú. 233 pp.

PRODUCE. 2013. Anuario estadístico pesquero y acuícola 2012. Ministerio de la Producción del Perú. 178 pp.

PRODUCE. 2014. Anuario estadístico pesquero y acuícola 2013. Ministerio de la Producción del Perú. 113 pp.

PRODUCE. 2015. Anuario estadístico pesquero y acuícola 2014. Ministerio de la Producción del Perú. 193 pp.

PRODUCE. 2016. Anuario estadístico pesquero y acuícola 2015. Ministerio de la Producción del Perú. 193 pp.

PRODUCE. 2017. Desenvolvimiento Productivo de la Actividad Pesquera. Boletín del sector Pesquero. Índice mayo 2017. Ministerio de la Producción del Perú. 44 pp.

Purca, S. 2005. Variabilidad de baja frecuencia en el Ecosistema de la Corriente Humboldt frente a Perú. Tesis de Doctorado. Universidad de Concepción, Chile.,

- Quispe-Ccalluari C., J. Tam, H. Demarcq, A. Chamorro, D. Espinoza-Morriberón, C. Romero, N. Dominguez, J. Ramos, R. Oliveros-Ramos, 2018. International Journal of Climatology. 1-10 p. DOI: 10.1002/joc.5493
- R Development Core Team. 2009. R: A language and environment for statistical computing. R Foundation for Statistical Computing, Vienna, Austria. ISBN 3-900051-07-0, URL <http://www.R-project.org>.
- Robinson, C.J., J. Gómez-Gutiérrez, U. Markaida & W. Gilly. 2016. Prolonged decline of jumbo squid (*Dosidicus gigas*) landings in the Gul of California is associated with chronically low wind stress and decreased chlorophyll a after El Niño 2009-2010. Fisheries Research 173. 128-138.
- Reynolds, R. W., T. S. Smith, C. Liu, D. B. Chelton, K. S. Casey, & M. G. Schlax. 2007. Daily high-resolution-blended analyses for sea surface temperature, J. Clim., 20, 5473–5496, doi:10.1175/2007JCLI1824.1.
- Ruiz-Cooley, R. I., D. Gendron, S. Aguñiga, S. Mesnick, & J. D. Carriquiry. 2004. Trophic relationships between sperm whales and jumbo squid using stable isotopes of C and N. Mar. Ecol. Prog. Ser. (277): 275–283.
- Schmiede, P. y E. Acuña. 1992. Regreso de las jibias (*Dosidicus gigas*) a Coquimbo. Revista Chilena de Historia Natural. 65:389-390.
- Staaf, DJ, Camarillo-Coop S, Haddock HD, Nyack AC & others. 2008. Natural egg mass deposition by the Humboldt squid (*Dosidicus gigas*) in the Gulf of California and characteristics of hatchlings and paralarvae. J. Mar. Biol. Assoc. UK. 88:759–770.
- Tafur, R., P. Villegas, M. Rabí & C. Yamashiro. 2001. Dynamics of maturation, seasonality of reproduction and spawning grounds of the jumbo squid *Dosidicus gigas* (Cephalopoda: Ommastrephidae) in Peruvian waters. Fisheries Research 54: 33-50.

- Taipe, A, C. Ymashiro, L. Mariategui, P. Rojas & C. Roque. 2001. Distribution and concentration of jumbo flying squid (*Dosidicus gigas*) off the Peruvian coast between 1991 and 1999. Fish. Res. 5:21-23.
- Tascheri R., P. Gálvez y J. Sateler. 2018.. Estatus y posibilidades de explotación. Convenio de Desempeño 2018. Estatus y posibilidades de explotación biológicamente sustentables de los principales recursos pesqueros nacionales, año 2019: Merluza común, 2019. Segundo Informe. Instituto de Fomento Pesquero.
- Wilhem, O. 1930. Las mortandades de jibias (*Omastrephe gigas*) en la Bahía de Talcahuano. Boletín de la Sociedad de Biología de Concepción (Chile). 3 - 14.
- Wilhem, O. 1951. Algunas observaciones acerca de las mortandades de jibias (*Dosidicus gigas* D'orb) en el litoral de concepción. Revista Chilena de Biología Marina Vol. IV. 196-201.
- Wolter, K. 1987. The Southern Oscillation in surface circulation and climate over the tropical Atlantic, Eastern Pacific, and Indian Oceans as captured by cluster analysis. J. Climate Appl. Meteor., 26: 540-558.
- Wormuth, J. H. 1976. The biogeography and numerical taxonomy of the oegopsid squid family Ommastrephidae in the Pacific Ocean. University of California Press. pp. 9–10.
- Zúñiga, M.J.; Cubillos, L.A. y Ibáñez, C. 2008. A regular pattern of periodicity in the monthly catch of jumbo squid (*Dosidicus gigas*) along the Chilean coast (2002-2005). Ciencias Marinas, 34: 91-99.

## LIST OF TABLES

Table 1. Results of the model of accumulated MEI.

Table 2. Correlations (Spearman) with their level of statistical significance between the monthly Humboldt Current Index (HCI) and the annual landings in all the EEZs, the annual landings in Chile, the length of maturity (L50%M) in Peru, the mantle length (median) in

Chile, and the weight at LM = 70cm in Chile. In the “r” column the colors indicate the relative magnitudes, while in the “p.value” column the green indicates when the correlation is significant (p.value <0.05).

Table 3. Results of the hierarchical model of the relation mantle length and total weights.

## LIST OF FIGURES

Figure 1. Species distribution of *Dosidicus gigas*. The historical distribution in red. The recent expansion and current condition in purple. Expansions to the south seem to have been more frequent than those to the north. Historical data mostly from Wormuth (1976).  
<http://tolweb.org>

Figure 2. Total HS landings by sector and annual catch quotas in Chile.

Figure 3. HS landings in the FAO area 87 by country and zone (ZEE: Exclusive Economic Zone; AI: International Waters). When a country fished in the EEZ of another country it is indicated, for example, as Japan\_ZEE.Peru. When the fishing zone is not differentiated, it is described as ZEE.AI, for example, Chile\_ZEE.AI.

Figure 4. Diagram of the functional triad of migration-maturation-growth (taken from Keyl *et al.*, 2008).

Figure 5. Model of the annual cycle of immigration and depletion of HS in San Antonio zone (30°S), based on standardized CPUE (taken from Payá 2014).

Figure 6. Growth model (thick black line) and monthly sizes structures in artisanal catches of San Antonio (brown line) from 2011 to 2013 (taken from Payá 2014).

Figure 7. HS relative abundance indices. CUPA obtained from bycatch of hake surveys and standardized CPUE of small and large fishing boats. The series were divided by their values in 2017 (taken from Payá 2019).

Figure 8. HS landings in Chile by fishing fleet.

Figure 9. HS landings in the FAO area 87 in EEZ and international waters (AI).

Figure 10. Comparison of MEI.ext, MEI.v1 and MEI.v2.

- Figure 11. Historical series of MEI, highlighting in green the years with HS straddling in beach and / or landings in Chile.
- Figure 12. Historical series of the accumulated MEI, and linear model (broken line). HS presence in Chile is highlighted in green.
- Figure 13. MEI and NOI, highlighting in green the HS presence in Chile.
- Figure 14. Coastal indices (ICEN, ITCP, HCI), highlighting in green the HS presence in Chile.
- Figure 15. Correlations between the HCI and HS landing in the EEZs of Chile, Peru and Ecuador.
- Figure 16. Correlations between the HCI and HS landing in the EEZ of Chile.
- Figure 17. HS landings of small boats by region and year (A) and proportion of their landing by month and year (B).
- Figure 18. HS landing of large boats by region and year (A) and proportion of their landing by month and year (B).
- Figure 19. HS fishing area of industrial trawler fleet during 2019, obtained from <https://globalfishingwatch.org/> (A) and the proportion of catches per month and year (B).
- Figure 20. Box-plot of HS sizes (ML) by year. A: Chilean commercial catches (own elaboration). B: bycatch of hydroacoustic hake surveys (taken from Molina and Rojas 2019).
- Figure 21. Median of HS sizes (ML) in commercial in Perú and in Chile and in the bycatch of hake surveys in Chile.
- Figure 22. Fits of hierarchical model of mantle length and weight of HS caught in Chile.
- Figure 23. Random errors parameters of hierarchical model of the mantle length and weight of HS caught in Chile.
- Figure 24. HS weights for 5 reference sizes (body condition), estimated using the hierarchical model of the mantle length and the weight of squid caught in Chile.
- Figure 25. Correlation between the Peruvian Oscillation Index (IOP) and the mantle length of 50% of maturity (L50M) in Peru (practically p-value =0).
- Figure 26. Correlations HCI and the mantle length of 50% of maturity (L50M) in Peru.
- Figure 27. Correlations between the October HCI and the mantle length of 50% of maturity (L50M) in Peru.

Figure 28. Correlations between the HCI and HS mantle length in Chile.

Figure 26. Correlations between HCI and body condition (weight of 70 cm ML) in Chile.

Figure 30. Anomalies of the ENSO indices region 3-4 and 1+2 and of the SST by degree of latitude between 1990 and 2018, for the zone 18-26°S and by three areas of different distance to the coast (0- 20 nm, 20-40 nm and 40-2000). Made by Adrian Bustamente (DOMA-IDOP).

Figure 31. Anomalies of the ENSO indices region 3-4 and 1 + 2 and of the SST by degree of latitude between 1990 and 2018, for the zone 25-33°S and by three areas of different distance to the coast (0- 20 nm, 20-40 nm and 40-2000). Made by Adrian Bustamente (DOMA-IDOP).

Figure 32. Anomalies of the ENSO indices region 3-4 and 1 + 2 and of the SST by degree of latitude between 1990 and 2018, for zone 32-41°S and by 3 areas of different distance to the coast (0- 20 nm, 20-40 nm and 40-2000). Made by Adrian Bustamente (DOMA-IDOP).

Figure 33. Time series for the period July 2002 - April 2019: a) Multivariate ENSO Index (MEI), lines: events declared El Niño (red) and La Niña (blue) and neutral (black). ATSM average (°C) between (18°-26°S, red) and (34°-40°S, blue) in the sector: b) coastal and c) oceanic. Average chlorophyll-a-satellite concentrations (µg/L) between (18°-26°S, red) and (34°-40°S, blue) in the sector: d) coastal and e) oceanic (taken from Angulo 2019).

Figure 34. Time series (September 2014-April 2019) in the Arica station: a) temperature (°C), b) salinity, c) dissolved oxygen concentration (mL/L) and d) chlorophyll (µg/L) (taken from Grendi *et al.*, 2019).

Figure 35. Time series (September 2014-April 2019) at the Iquique station: a) temperature (°C), b) salinity, c) dissolved oxygen concentration (mL / L) and d) chlorophyll (µg/L) (taken from Grendi *et al.*, 2019).

Figure 36. Time series (September 2014-April 2019) at the Mejillones station: a) temperature (°C), b) salinity, c) dissolved oxygen concentration (mL / L) and d) chlorophyll (µg / L) (taken from Grendi *et al.*, 2019).

Figure 37. Time series (October 2014-April 2019) at the fixed stations of Coliumo at 5 nm, 12 nm and 18 nm from the coast: a) temperature ( $^{\circ}\text{C}$ ), b) salinity, c) density ( $\text{kg}/\text{m}^3$ ) (taken from Grendi *et al.*, 2019).

Figure 38. Time series (October 2014-April 2019) at the fixed stations of Coliumo at 12 nm from the coast: a) temperature ( $^{\circ}\text{C}$ ), b) salinity, c) density ( $\text{kg} / \text{m}^3$ ) (taken from Grendi *et al.*, 2019).

Figure 39. Time series (October 2014-April 2019) at the fixed stations of Coliumo at 18 nm from the coast: a) temperature ( $^{\circ}\text{C}$ ), b) salinity, c) density ( $\text{kg} / \text{m}^3$ ) (taken from Grendi *et al.*, 2019).

Figure 40. Time series (January 2016-March 2019) at the Corral station 10 nm from the coast: a) temperature ( $^{\circ}\text{C}$ ), b) salinity, c) density ( $\text{kg} / \text{m}^3$ ) (taken from Grendi *et al.*, 2019).

Figure 41. Latitudinal oceanographic sections of temperature ( $^{\circ}\text{C}$ ), salinity (psu) and concentration of dissolved oxygen ( $\text{ml}/\text{L}$ ) in the south-central area (taken from Angulo *et al.*, 2018).

Figure 42. Chlorophyll profiles by latitude and depth in 2016 and 2017, and surface chlorophyll-a concentration in 2018 during the July-August hake surveys (taken from Angulo *et al.*, 2017, 2018 and 2019). Note that in 2016 and 2017 the scale is in  $\text{ml}/\text{L}$  and in 2019 in  $\text{mg}/\text{m}^3$ .



## TABLES

TABLE 1

Name	Period	Estimate	Gradient
Rate1	<1925	-0.19	-0.02
Rate2	1925-1942	0.27	0.04
Rate3	1943-1976	-0.13	0.01
Rate4	1977-1998	0.24	0.00
Rate5	1999-2015	-0.33	0.03
Rate6	>2015	0.19	-0.02
MEIA	1871	-28.33	0.00

TABLE 2

Month	Landing in all EEZs			Landing in Chilean EEZ			L50%M in Perú			ML in Chile			Weight_70 in Chile		
	r	p.value		r	p.value		r	p.value		r	p.value		r	p.value	
1	0.52	4.6E-04		0.53	3.3E-04		0.43	1.7E-02		0.24	3.2E-01		0.21	5.9E-01	
2	0.58	6.5E-05		0.54	2.5E-04		0.48	6.9E-03		0.29	2.3E-01		0.64	6.3E-02	
3	0.64	7.0E-06		0.63	1.1E-05		0.54	2.0E-03		0.07	7.9E-01		0.15	7.1E-01	
4	0.63	9.3E-06		0.56	1.4E-04		0.56	1.3E-03		0.22	3.7E-01		0.38	3.1E-01	
5	0.46	2.5E-03		0.41	7.6E-03		0.39	3.4E-02		-0.11	6.6E-01		-0.20	6.0E-01	
6	0.51	7.4E-04		0.47	1.9E-03		0.32	8.9E-02		0.05	8.4E-01		0.69	4.1E-02	
7	0.59	5.3E-05		0.53	3.9E-04		0.34	6.8E-02		0.14	5.8E-01		0.34	4.1E-01	
8	0.60	3.3E-05		0.51	7.2E-04		0.42	2.0E-02		0.34	1.7E-01		0.28	5.0E-01	
9	0.63	1.1E-05		0.58	6.8E-05		0.44	1.5E-02		0.14	5.8E-01		0.50	2.1E-01	
10	0.70	2.9E-07		0.68	1.0E-06		0.60	4.2E-04		0.45	6.1E-02		-0.43	2.9E-01	
11	0.68	8.8E-07		0.61	1.9E-05		0.41	2.5E-02		0.51	2.9E-02		0.57	1.4E-01	
12	0.61	2.6E-05		0.55	1.9E-04		0.46	1.1E-02		0.50	3.6E-02		0.36	3.8E-01	

TABLE 3

HiperParameters				
logsigma	mean_log_a	sigma_log_a	mean_log_b	sigma_log_b
-2.005401	-11.0530579	0.80212216	1.15396517	0.06106218
Rnandom Errors				
log_a_2011	-9.246883			
log_a_2012	-11.098287			
log_a_2013	-11.737294			
log_a_2014	-11.706171			
log_a_2015	-11.528831			
log_a_2016	-10.874753			
log_a_2017	-10.919413			
log_a_2018	-11.96948			
log_a_2019	-10.403173			
log_b_2011	1.022675			
log_b_2012	1.161175			
log_b_2013	1.210078			
log_b_2014	1.203302			
log_b_2015	1.189868			
log_b_2016	1.14211			
log_b_2017	1.143982			
log_b_2018	1.222257			
log_b_2019	1.091015			

## FIGURES

FIGURE 1

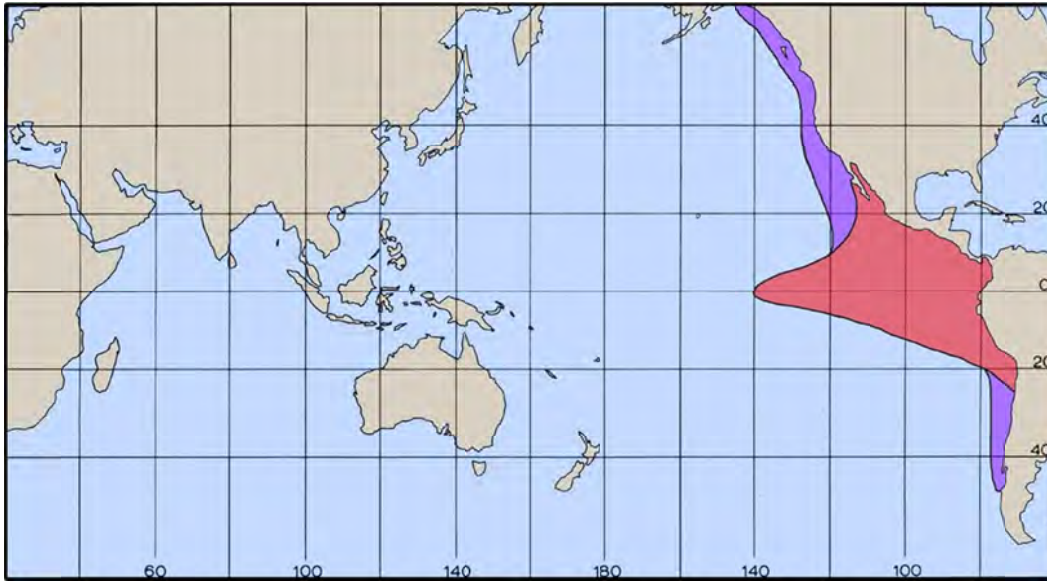


FIGURE 2

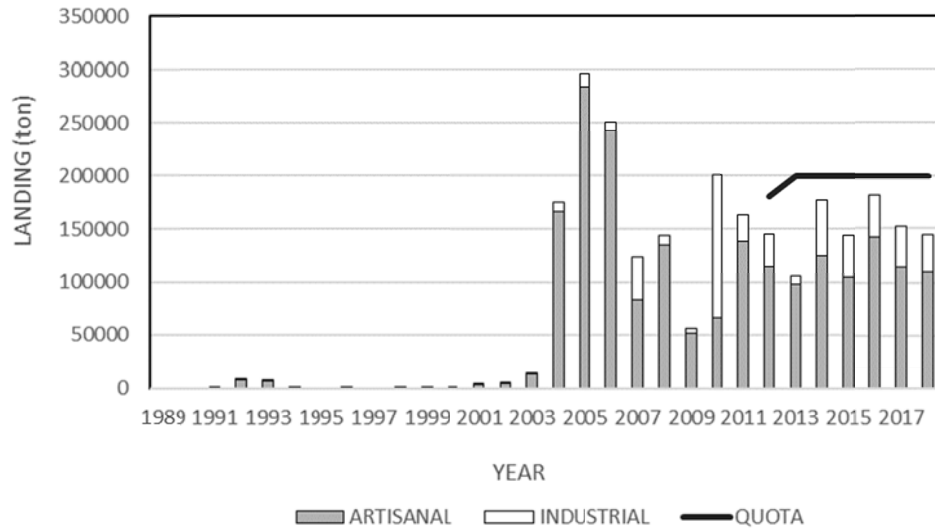


FIGURE 3

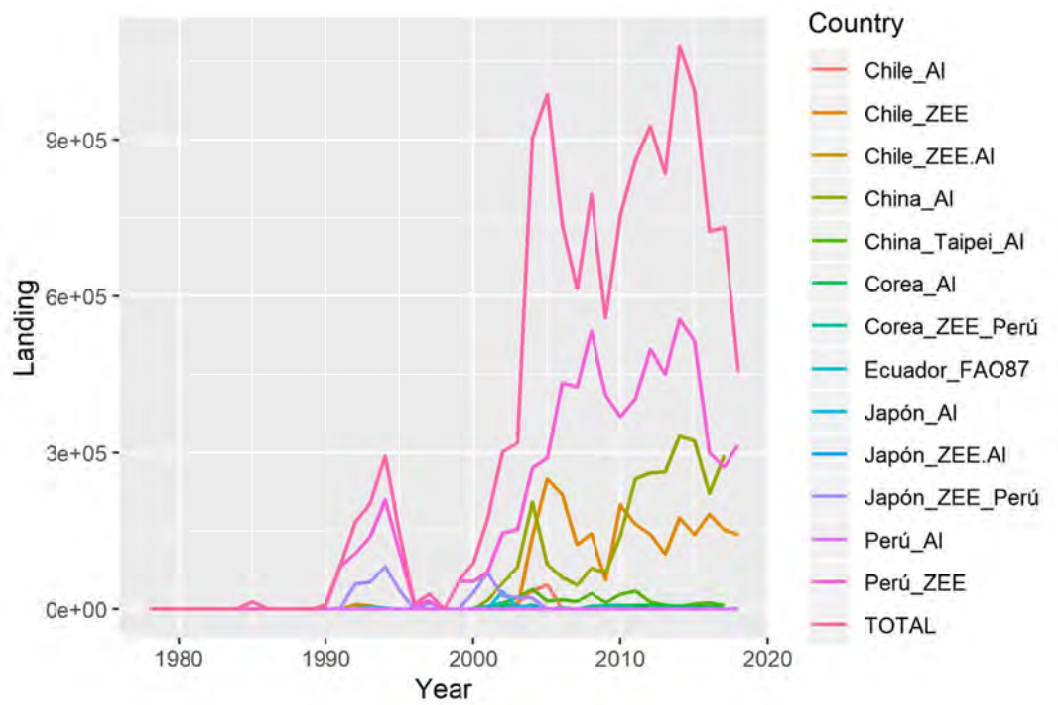


FIGURE 4

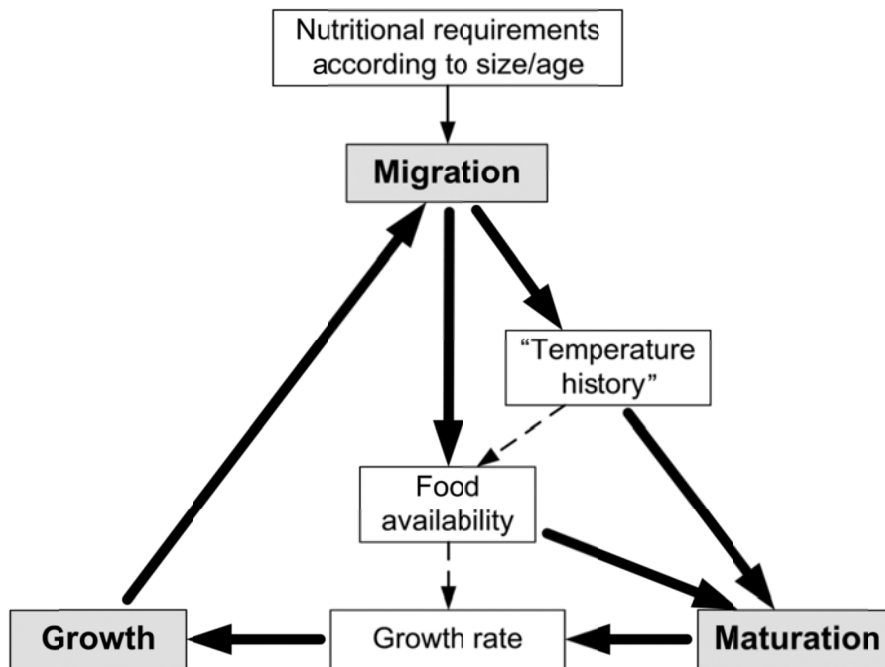


FIGURE 5

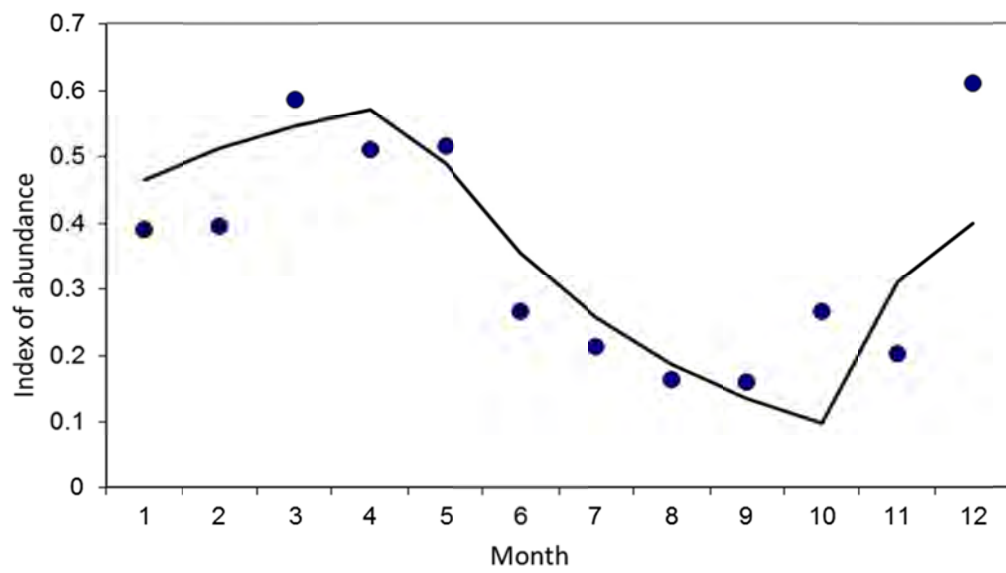




FIGURE 6.

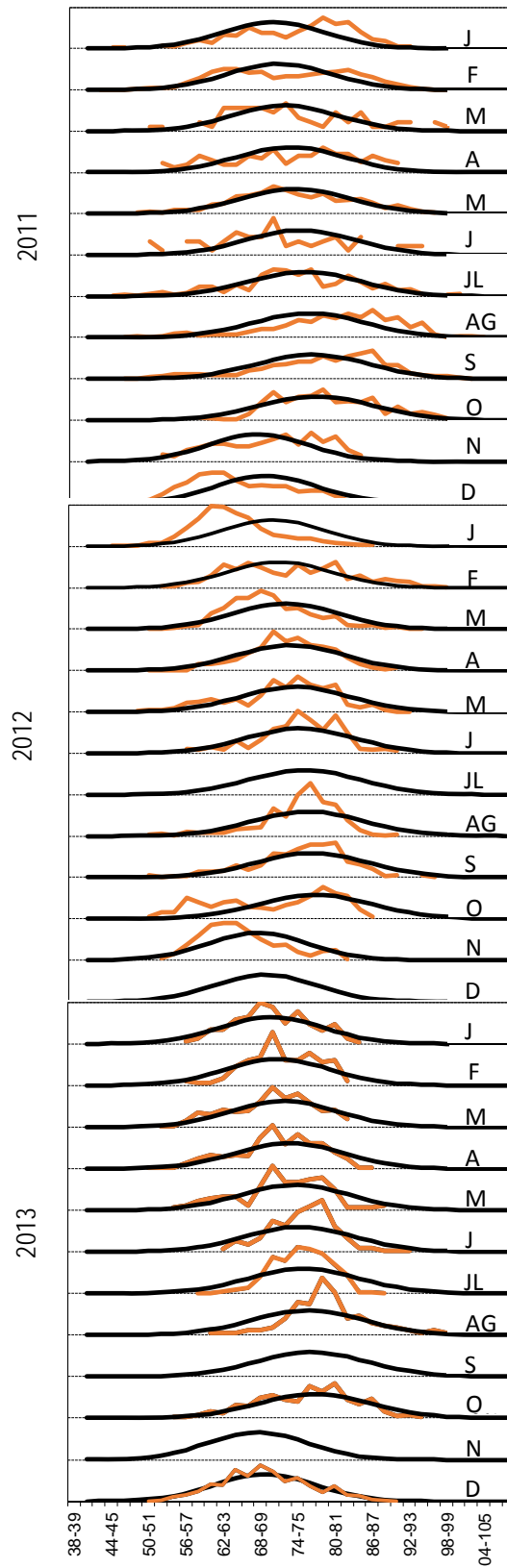


FIGURE 7.

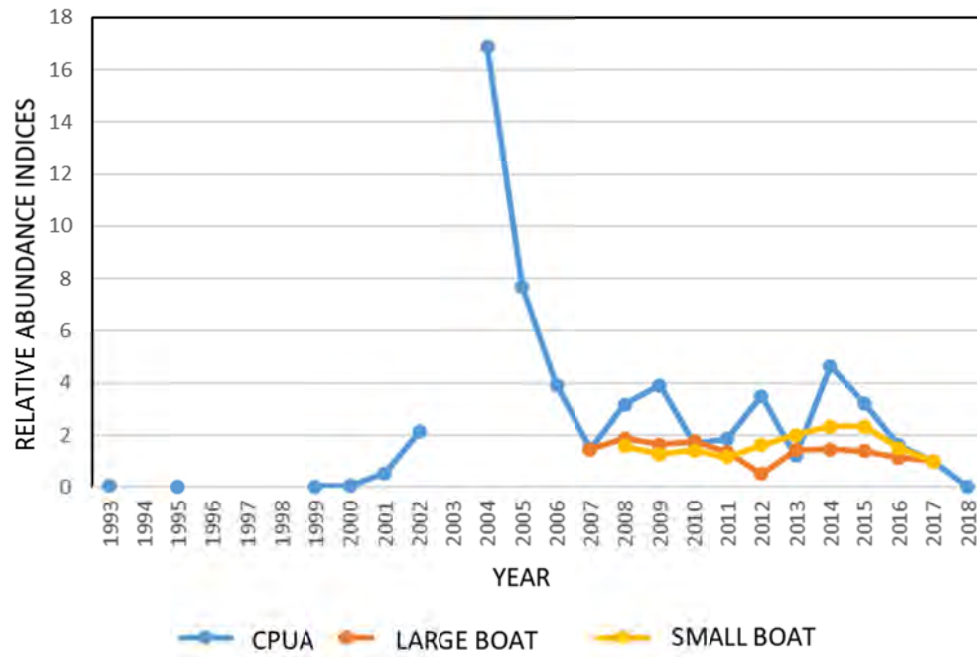


FIGURE 8

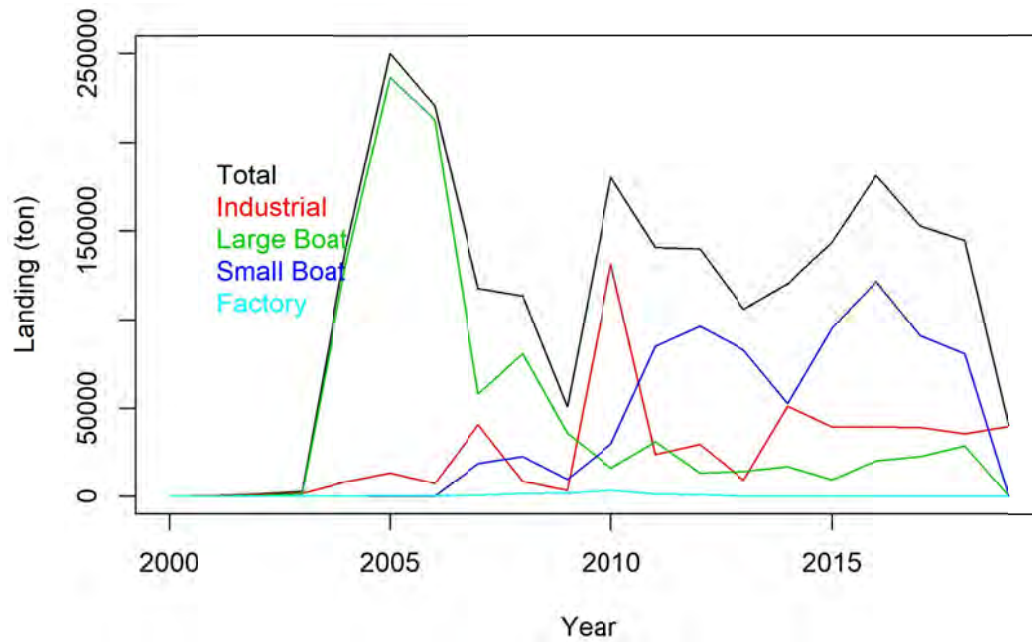


FIGURE 9.

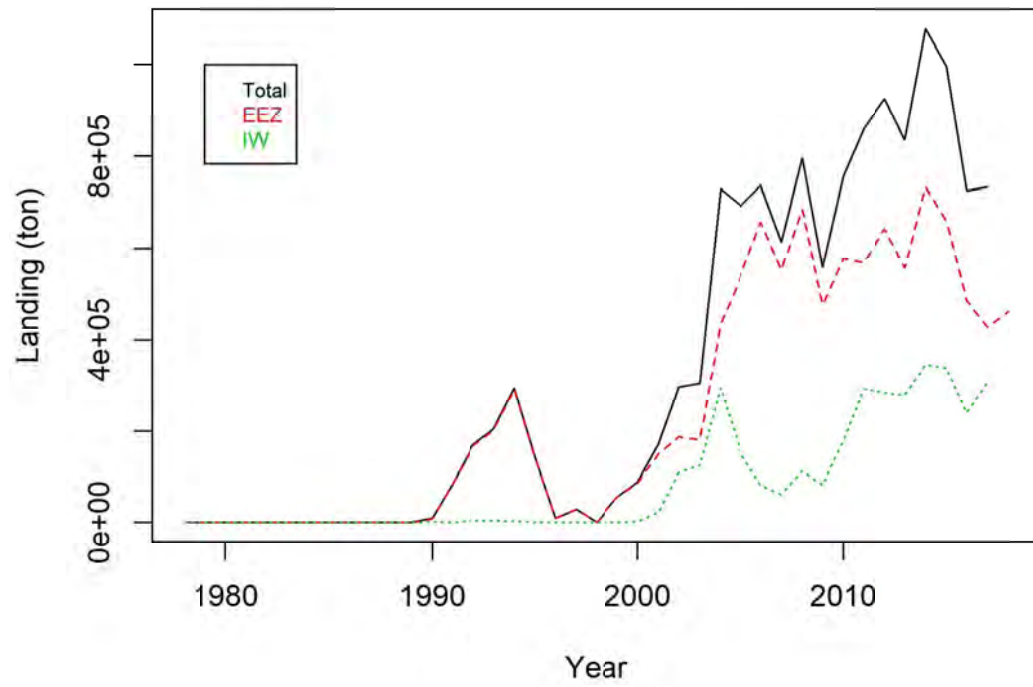


FIGURE 10

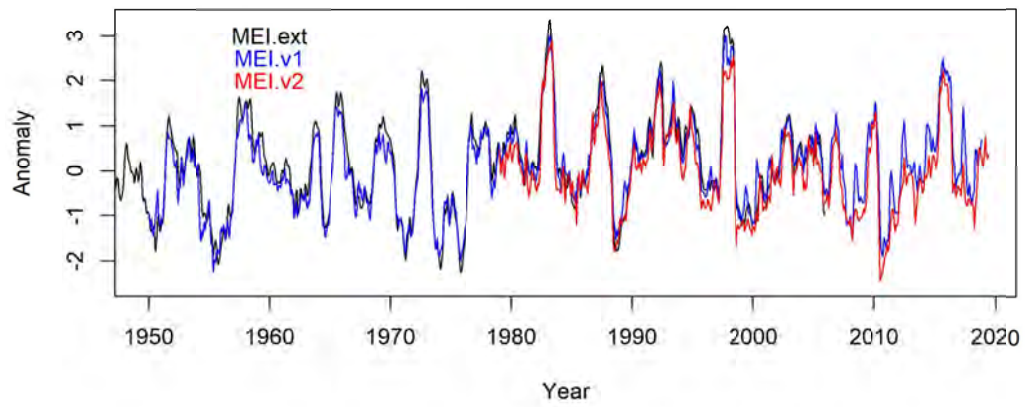


FIGURE 11

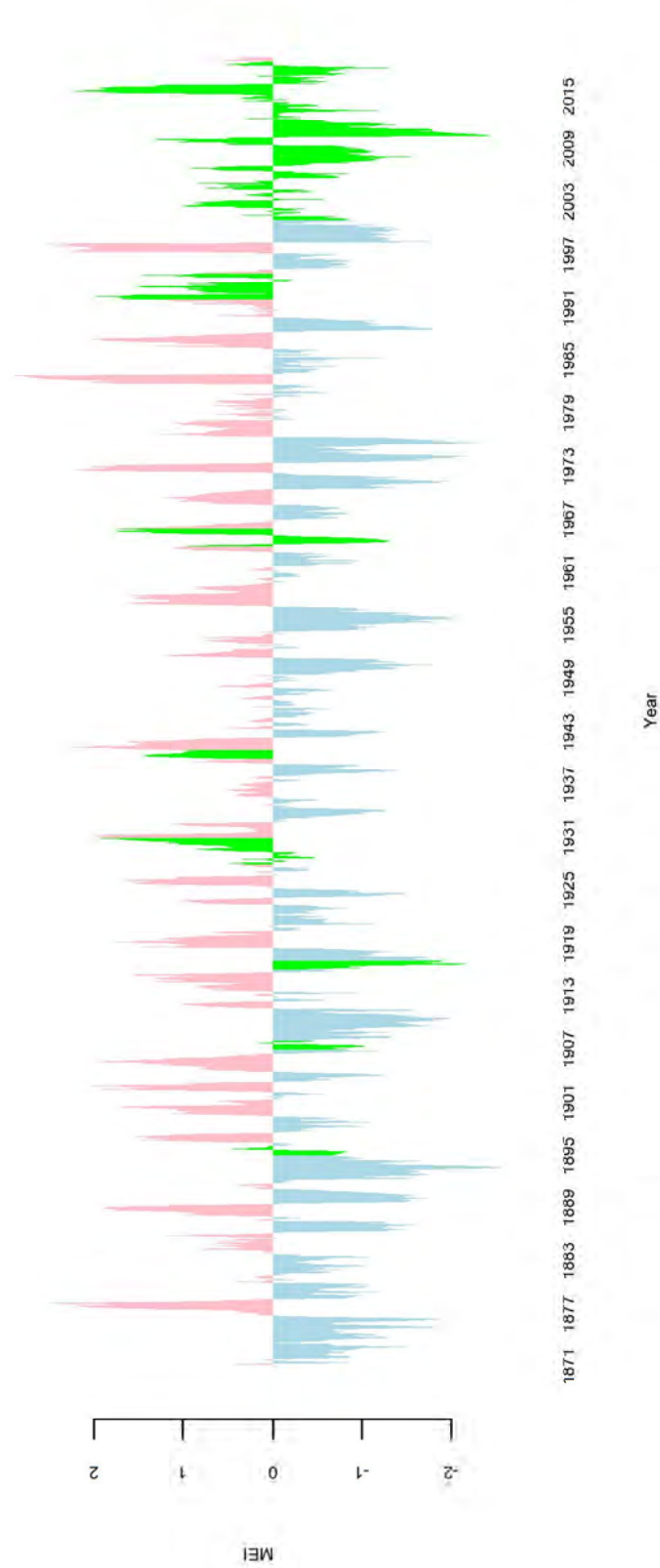


FIGURE 12

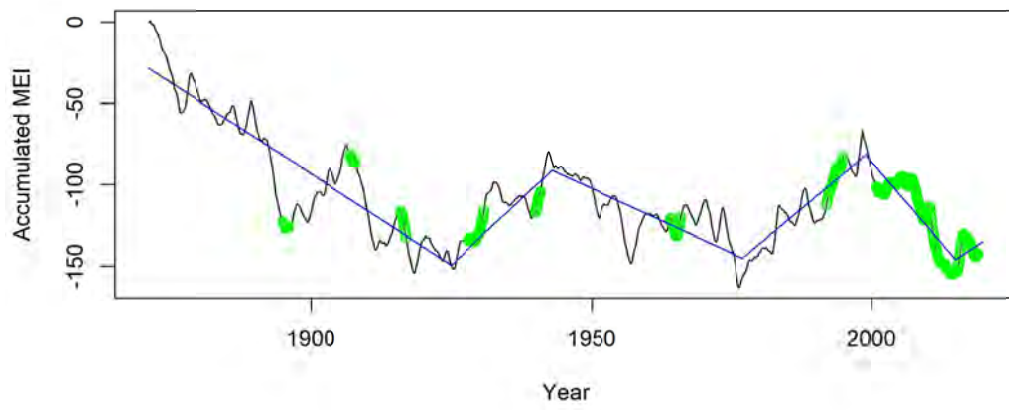


FIGURE 13

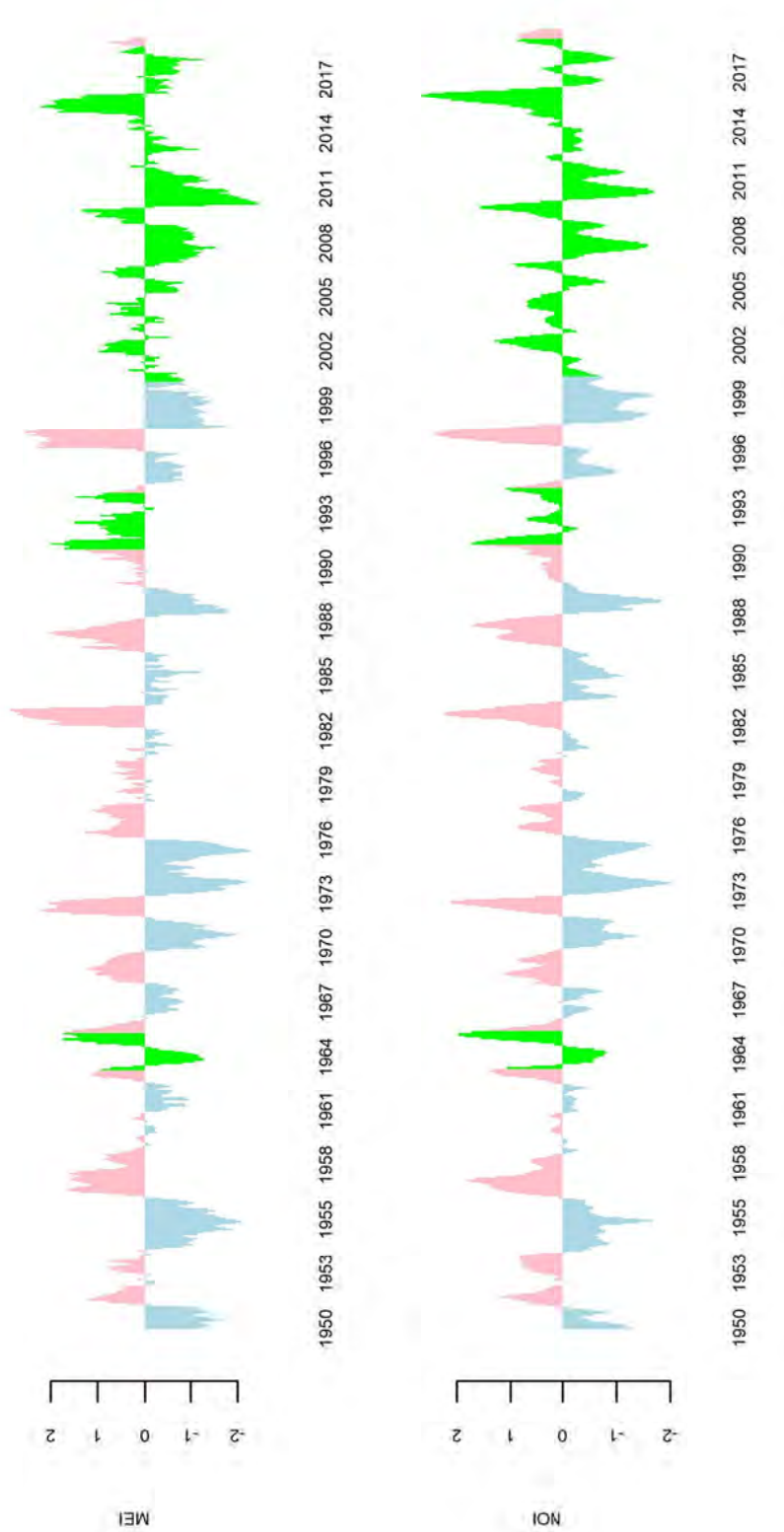




FIGURE 14

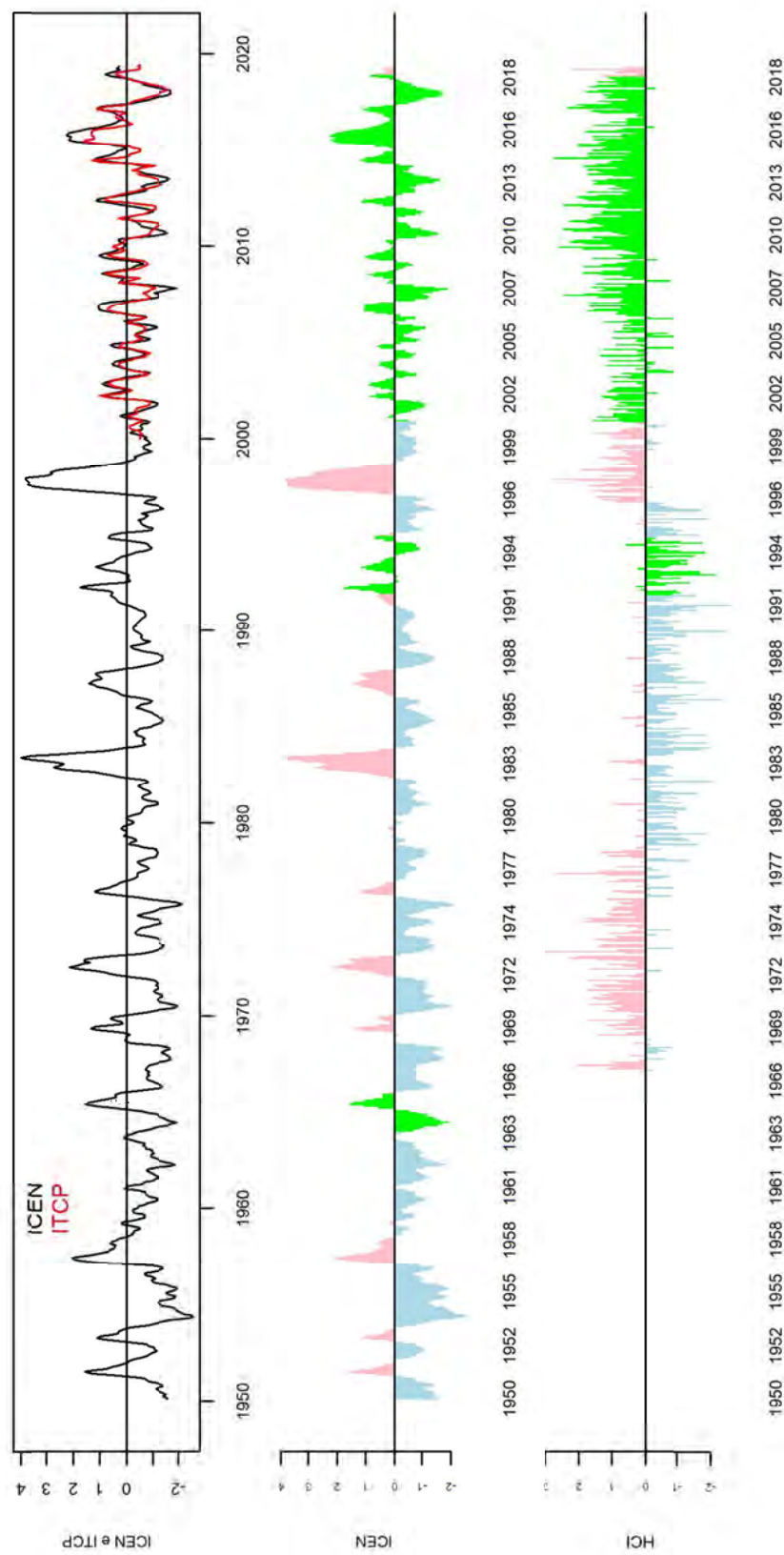


FIGURA 15

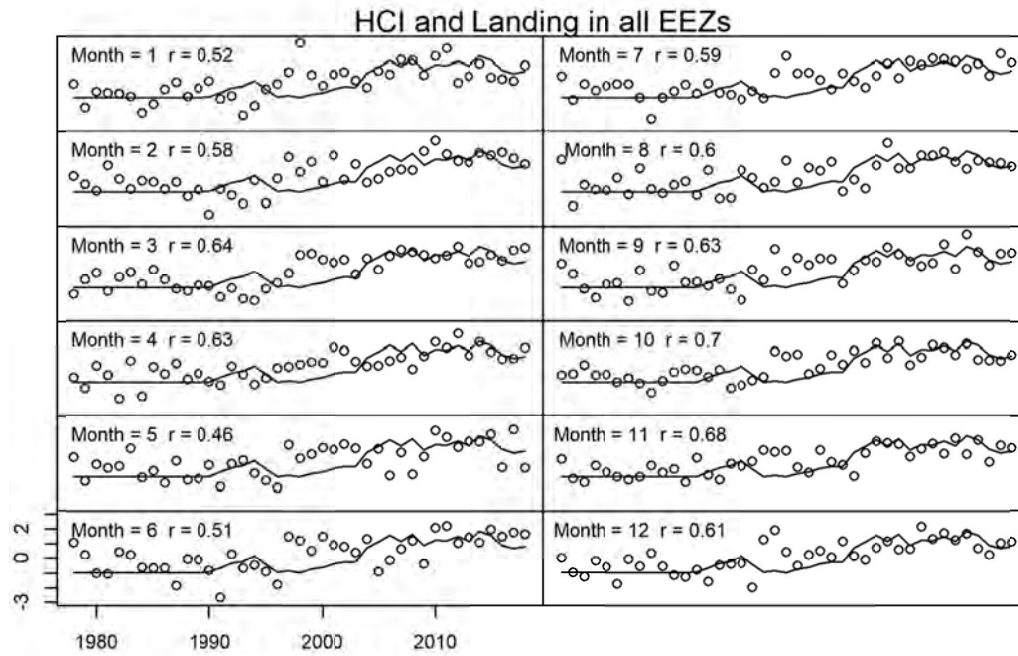


FIGURE 16

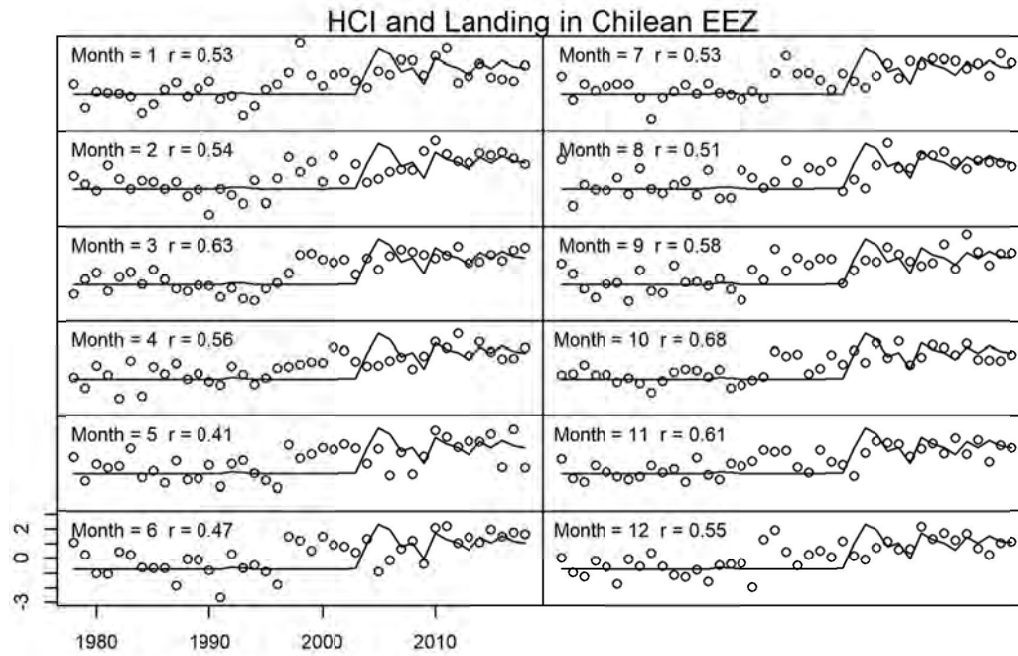
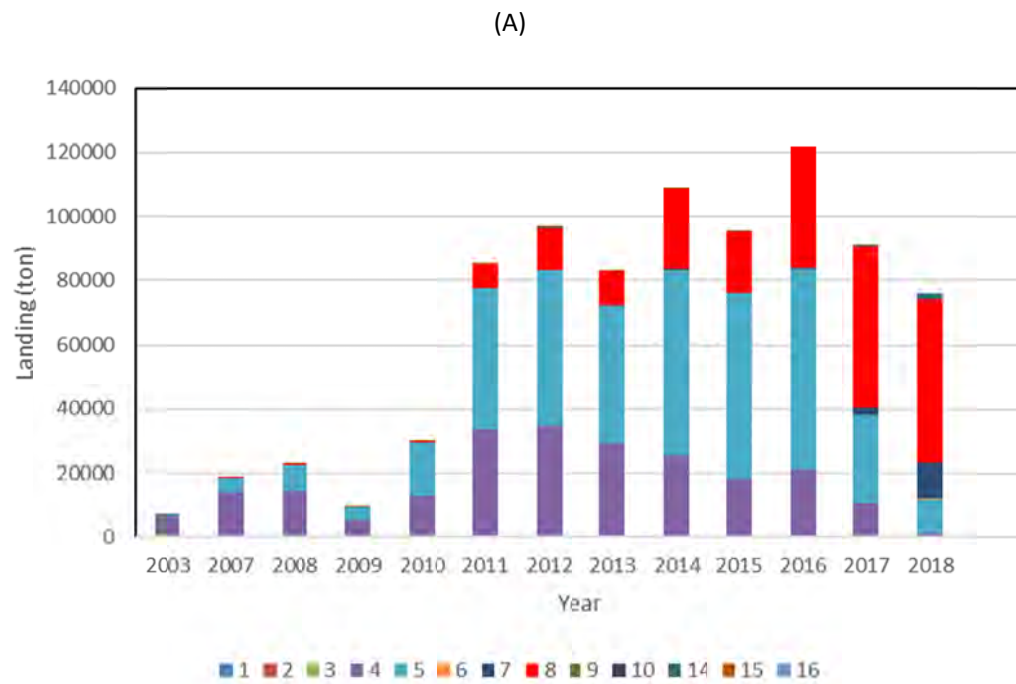


FIGURE 17



(B)

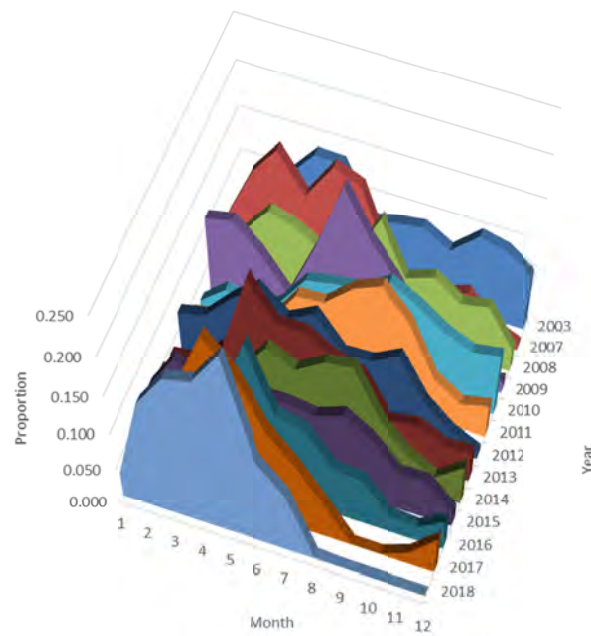


FIGURE 18

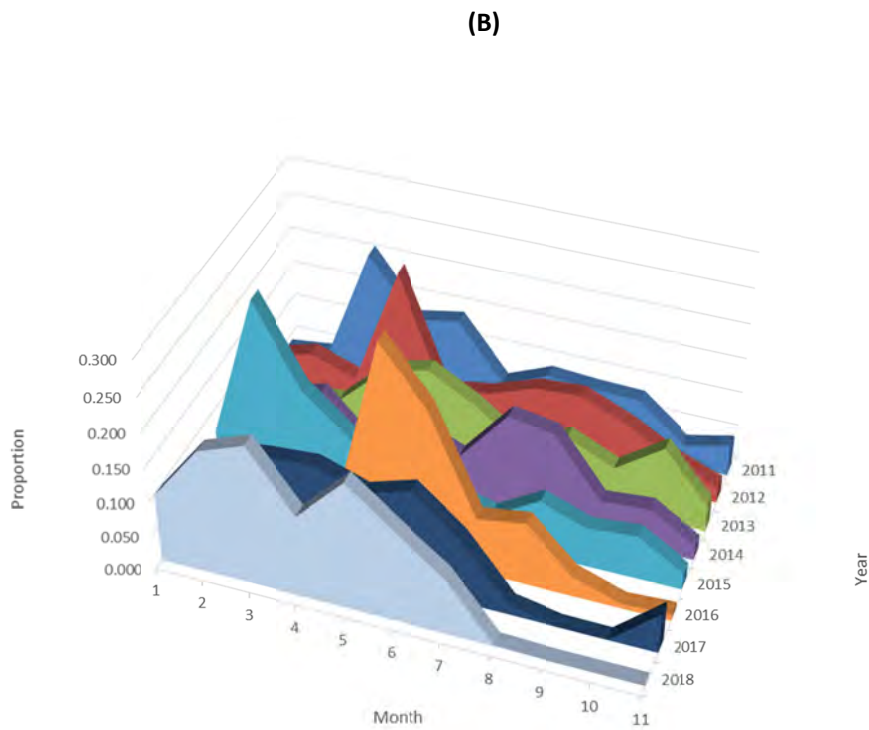
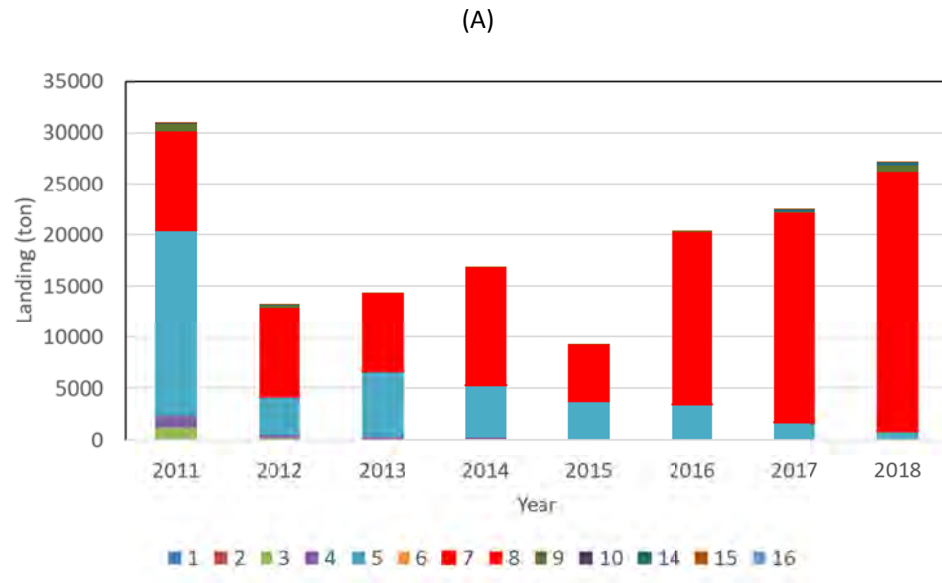
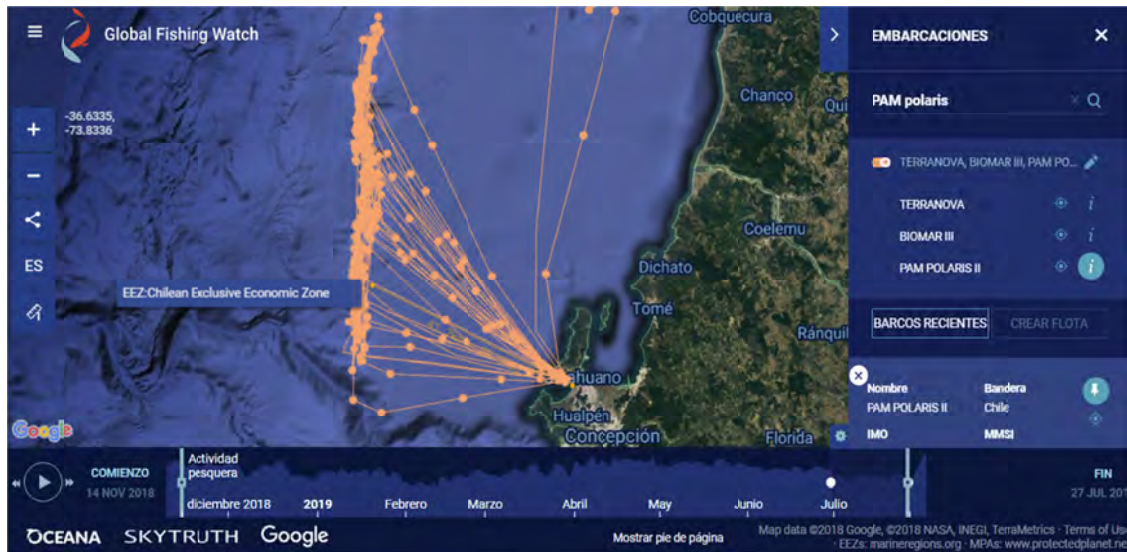


FIGURE 19.

(A)



(B)

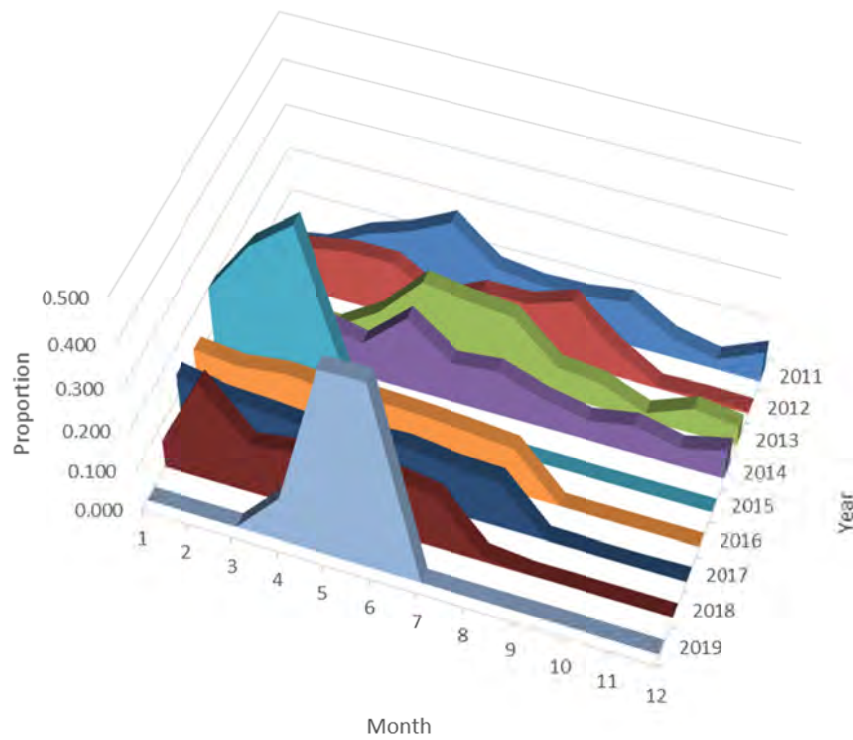




FIGURE 20

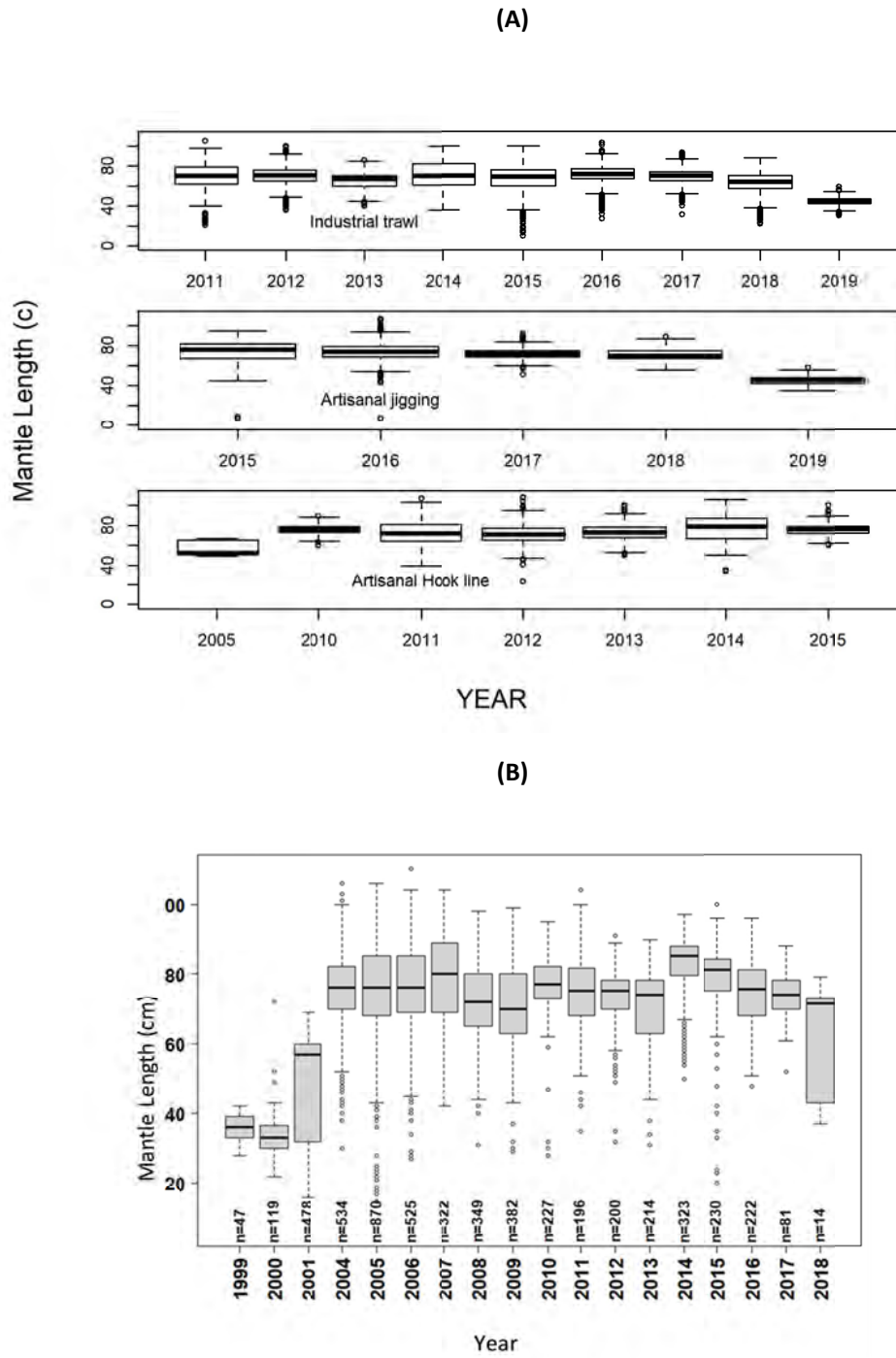


FIGURE 21

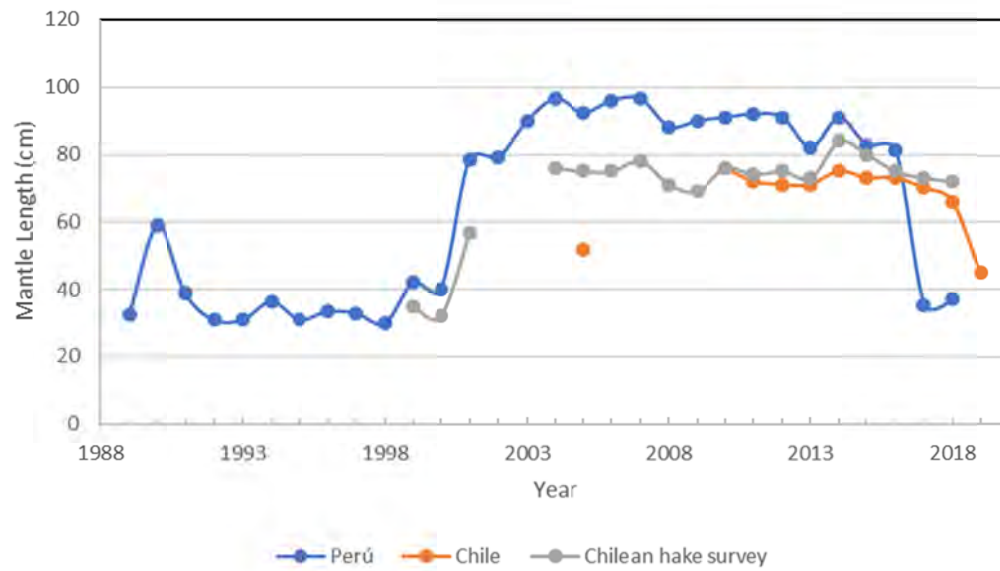




FIGURE 22

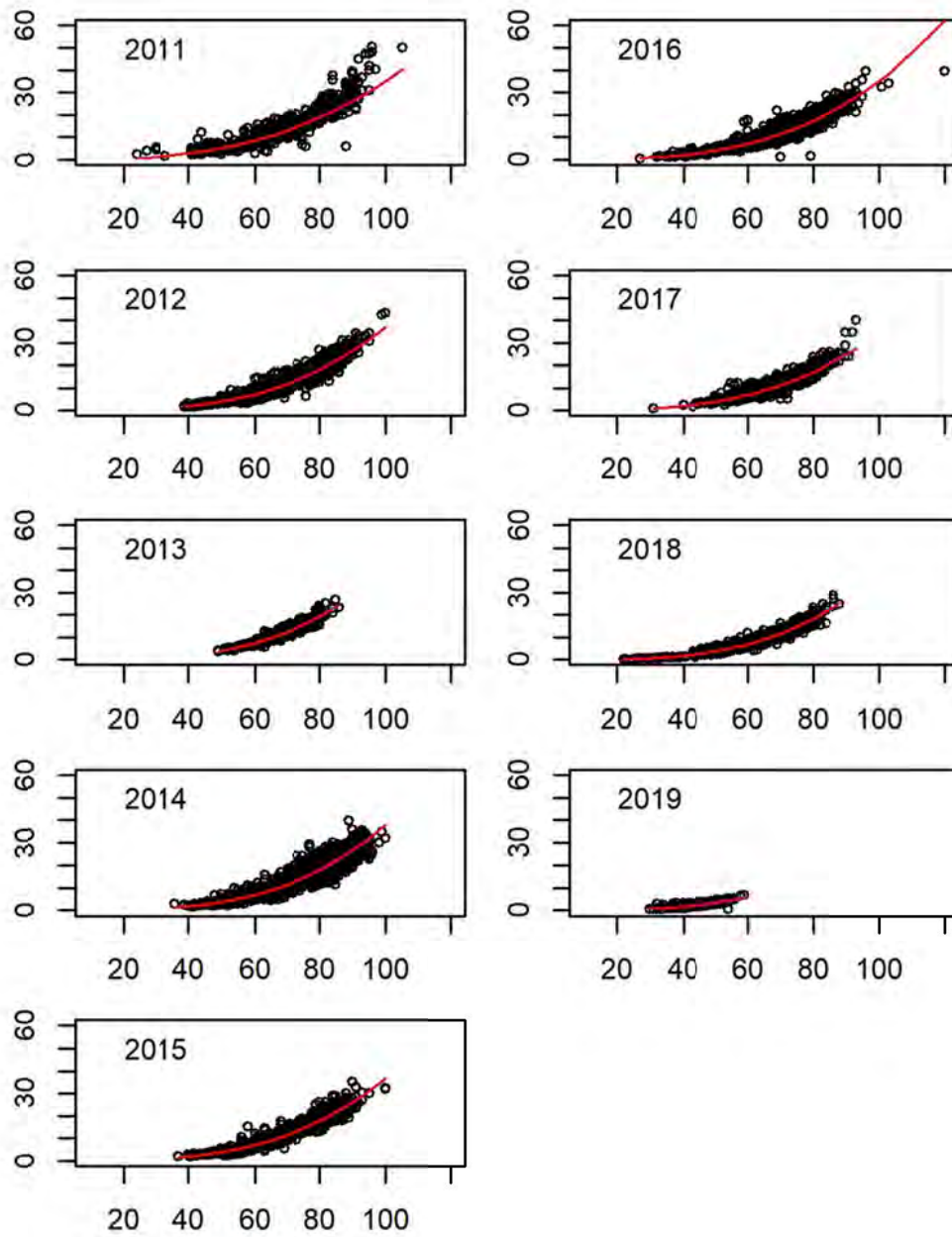


FIGURE 23

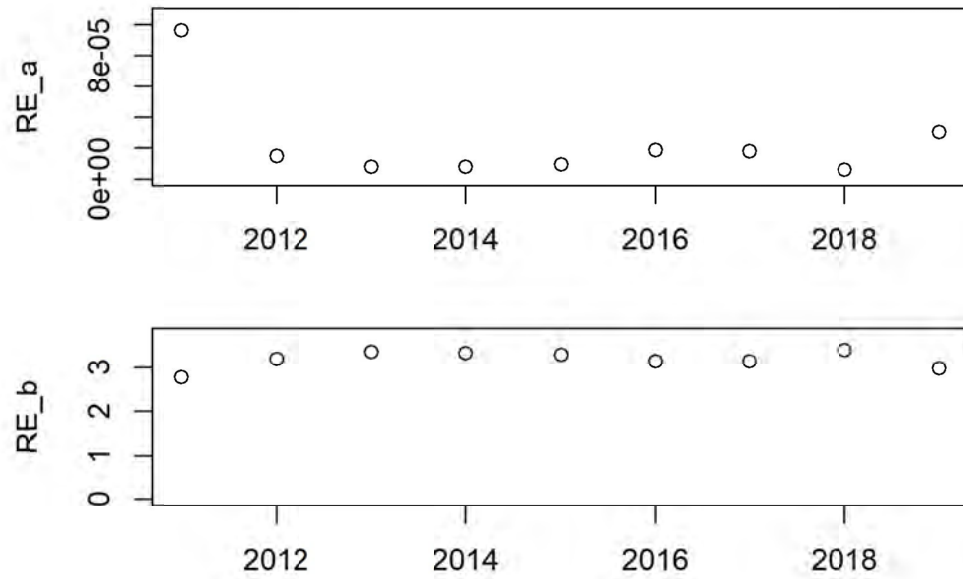


FIGURE 24

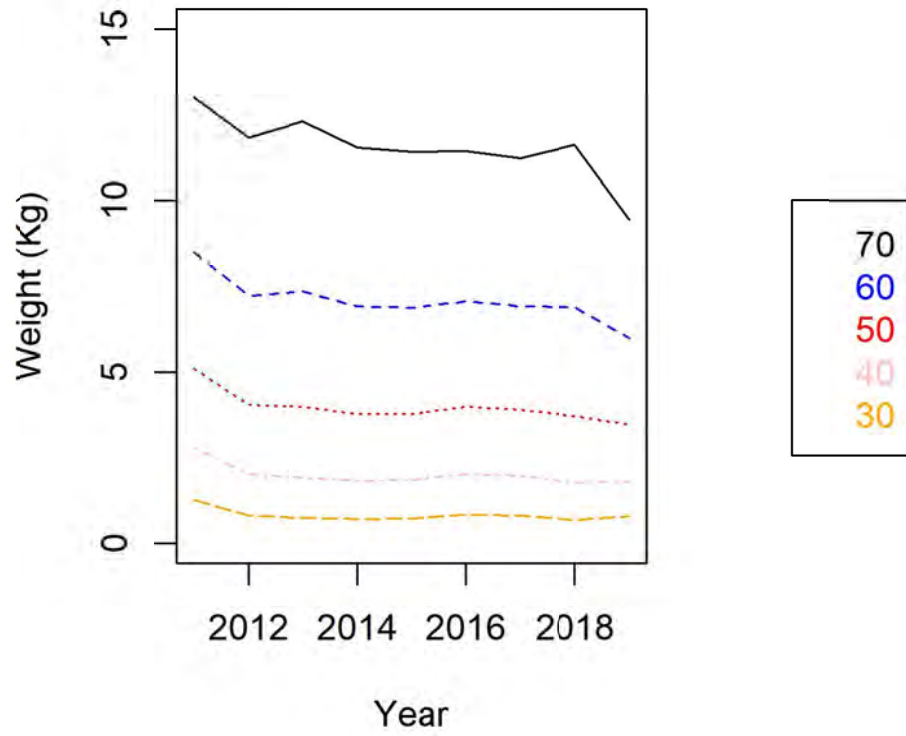


FIGURE 25

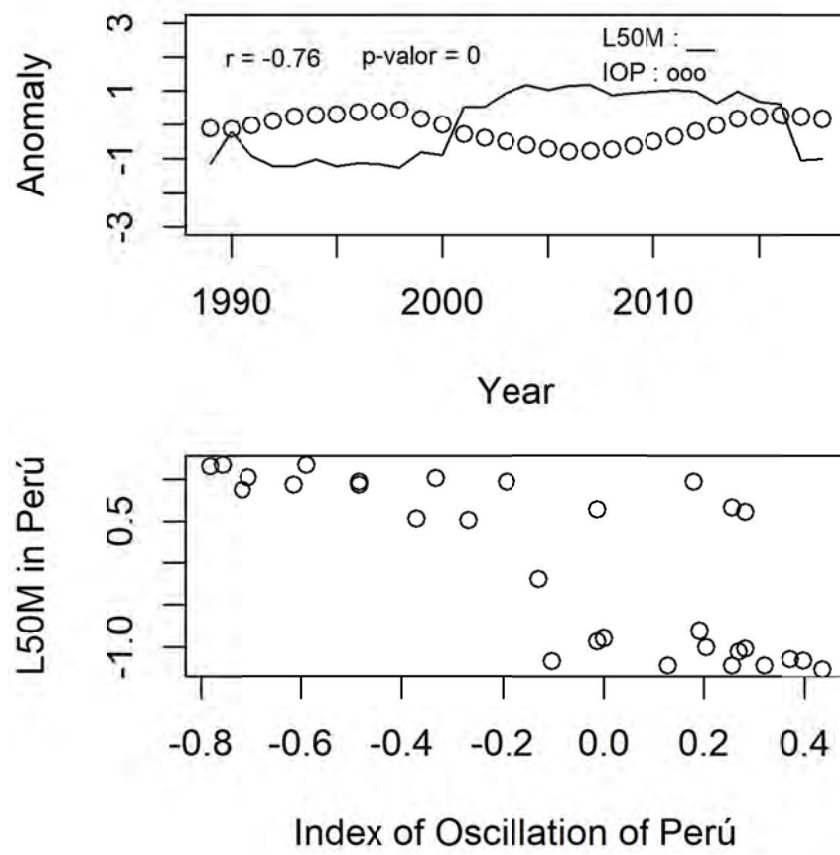


FIGURE 26

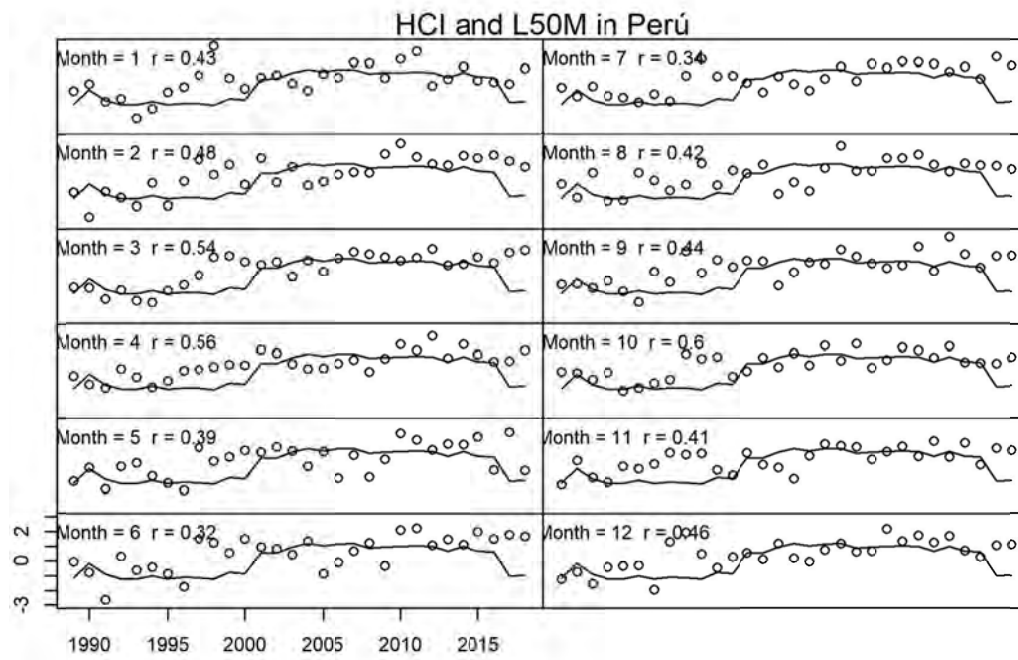


FIGURE 27

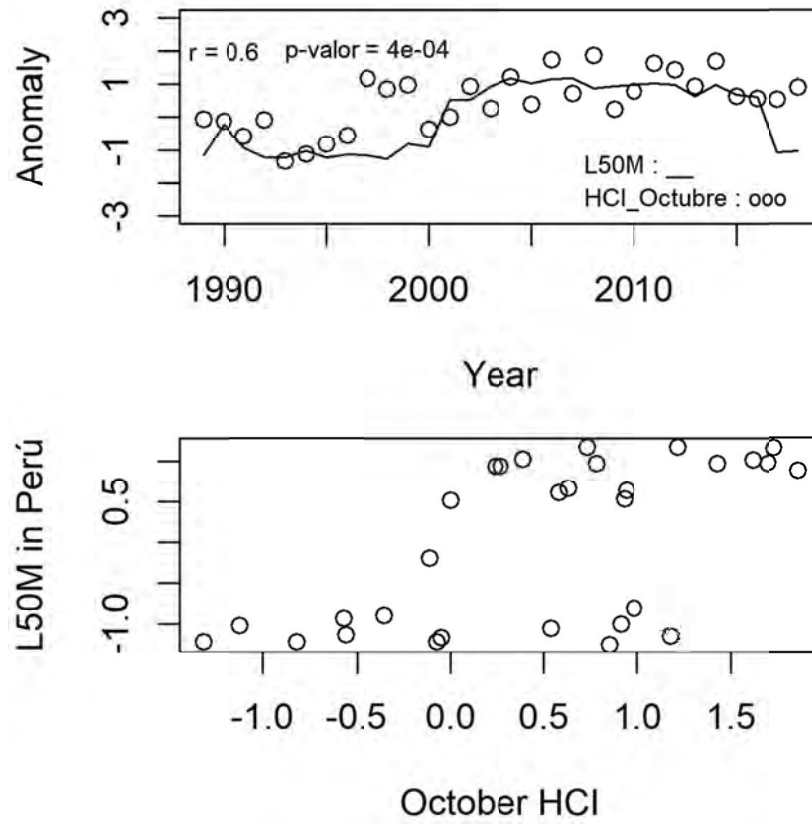


FIGURE 28

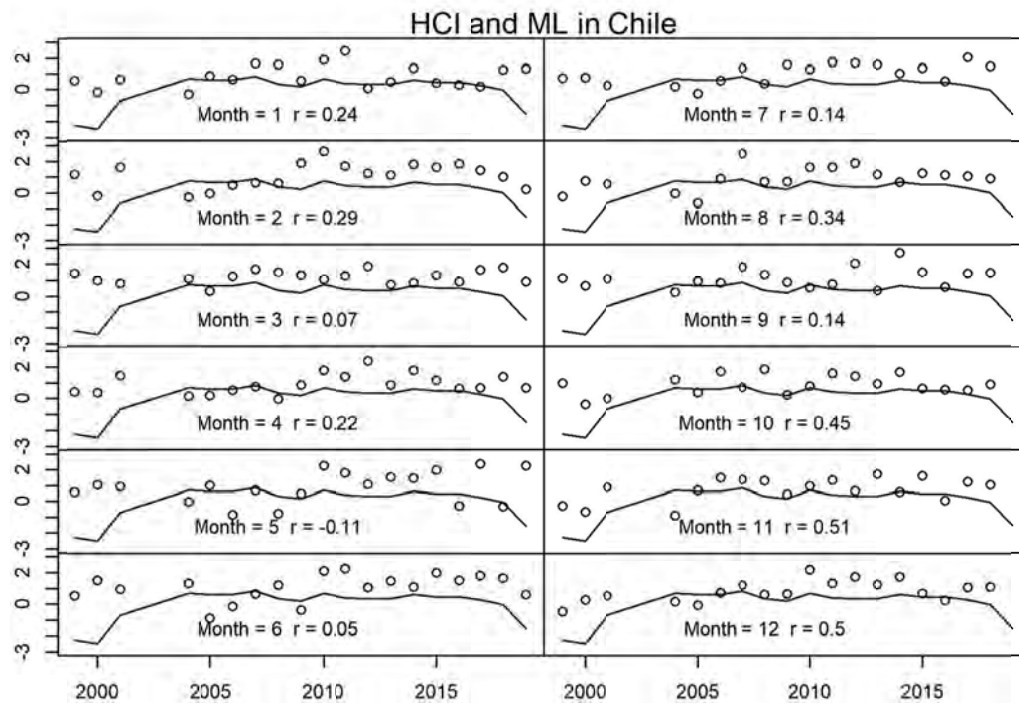


FIGURE 29

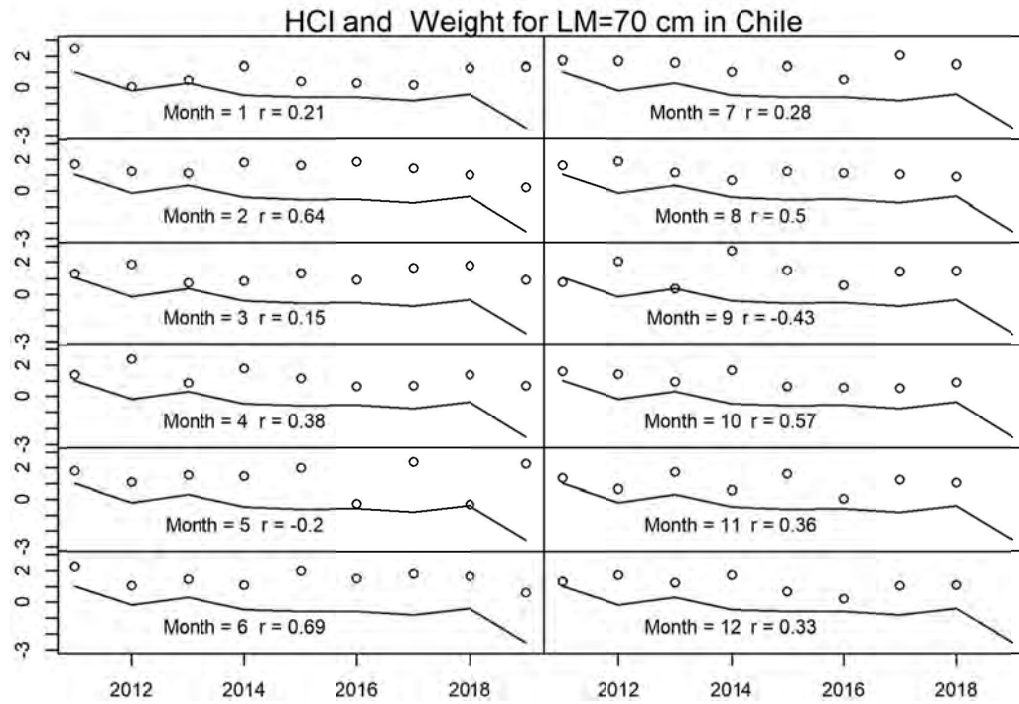




FIGURE 30

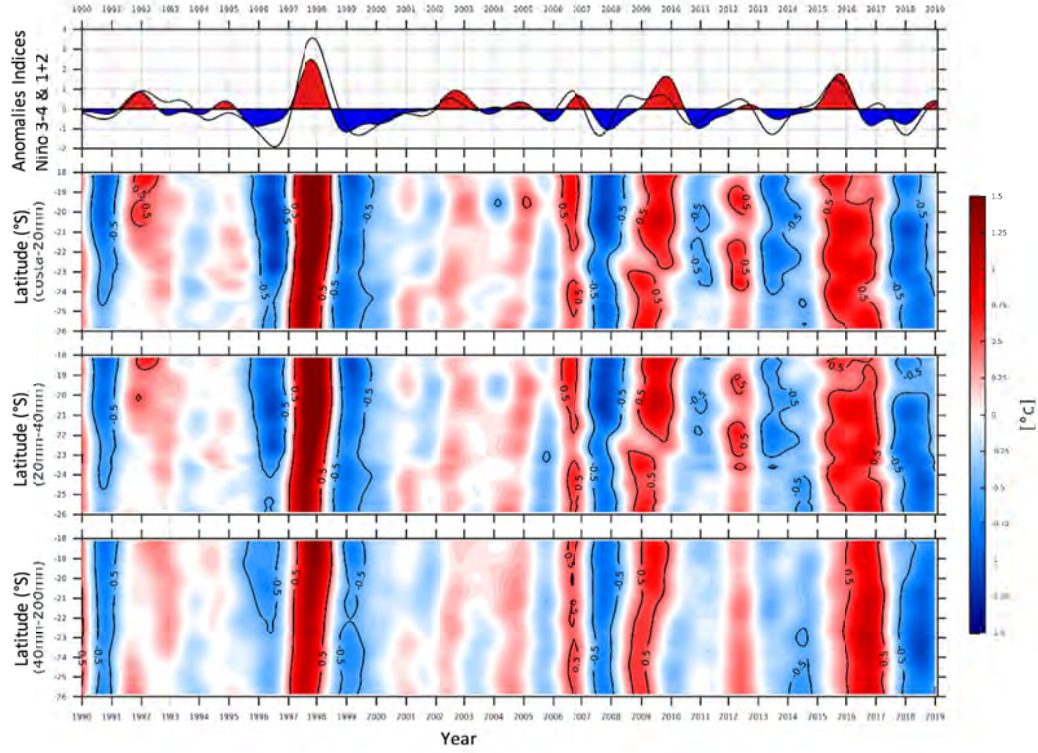


FIGURE 31

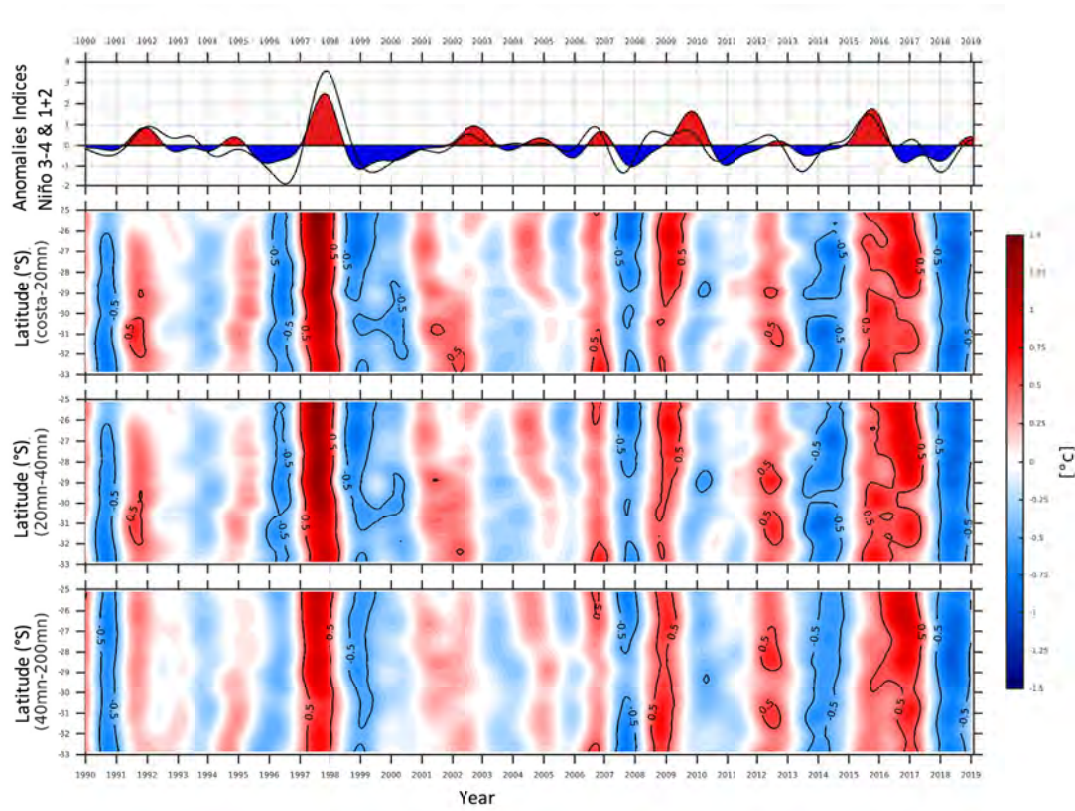


FIGURE 32

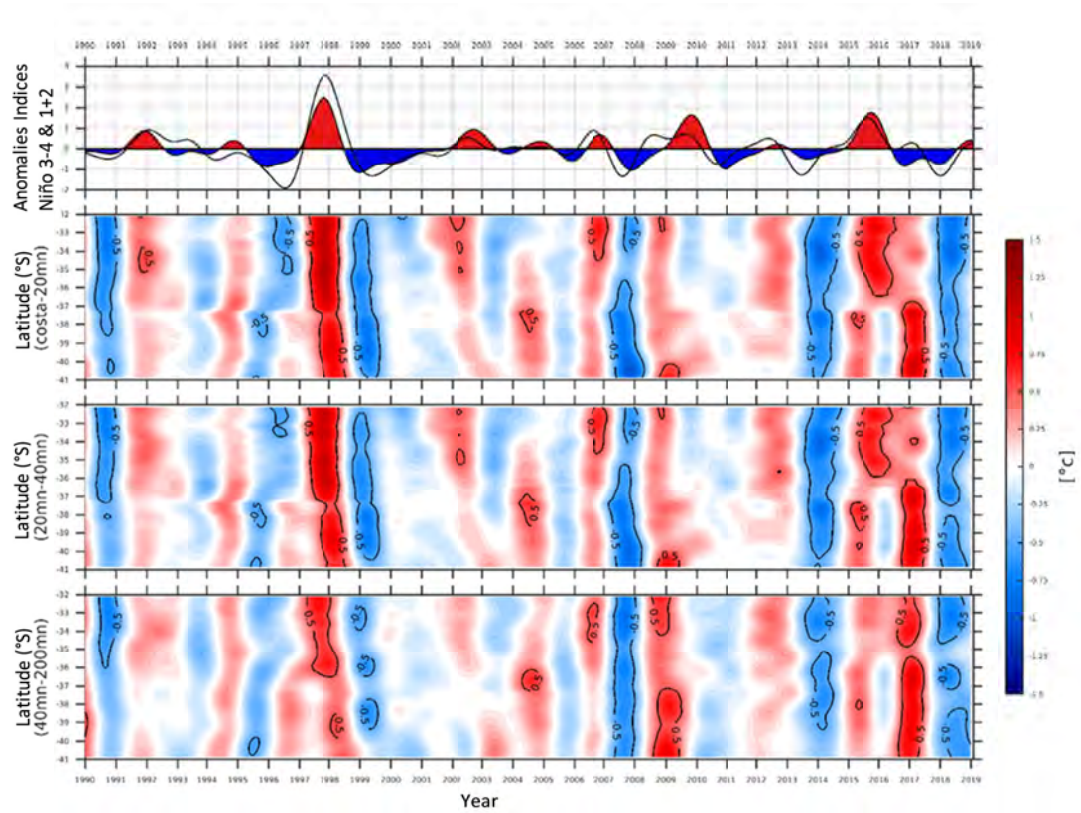




FIGURE 33

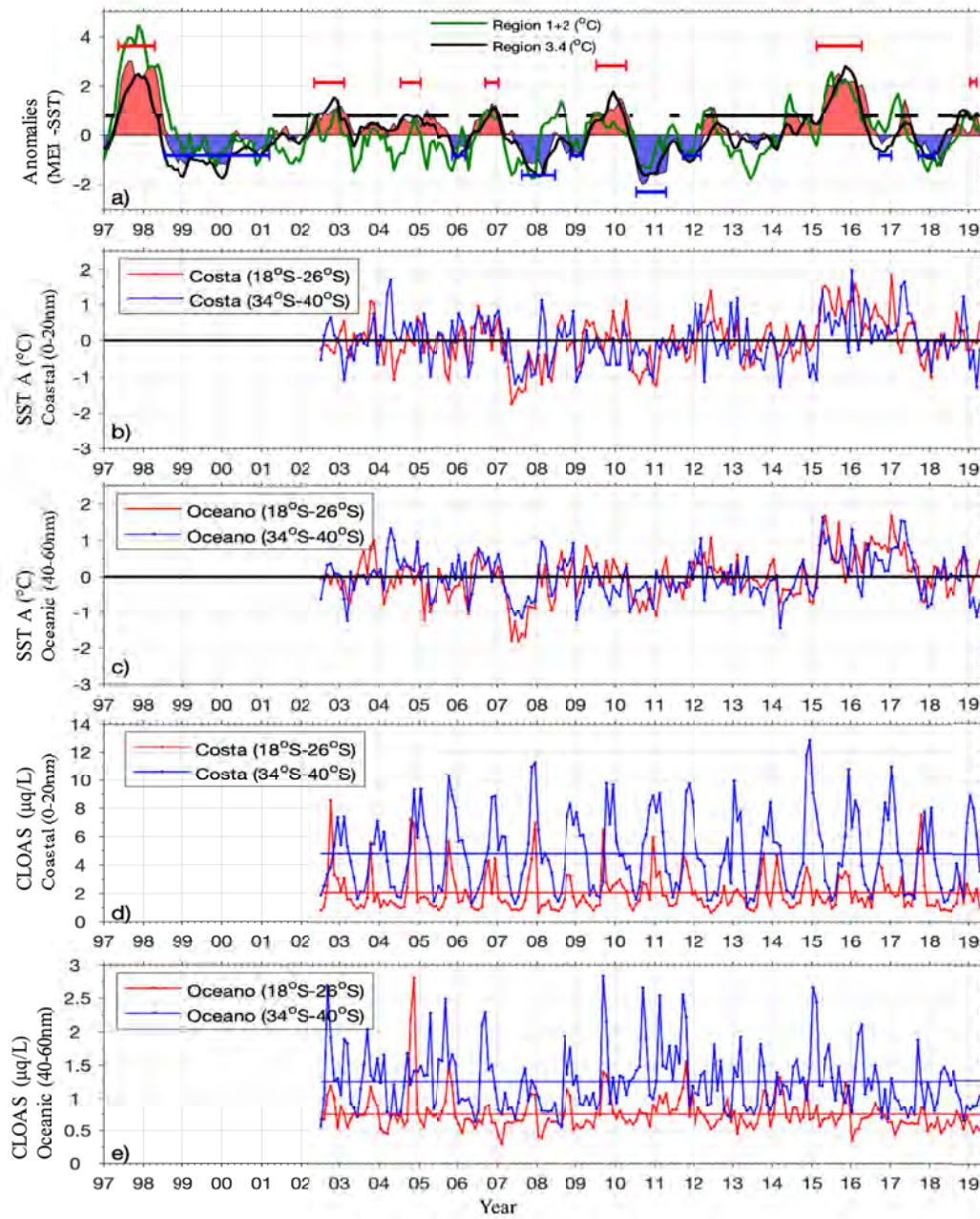


FIGURE 34

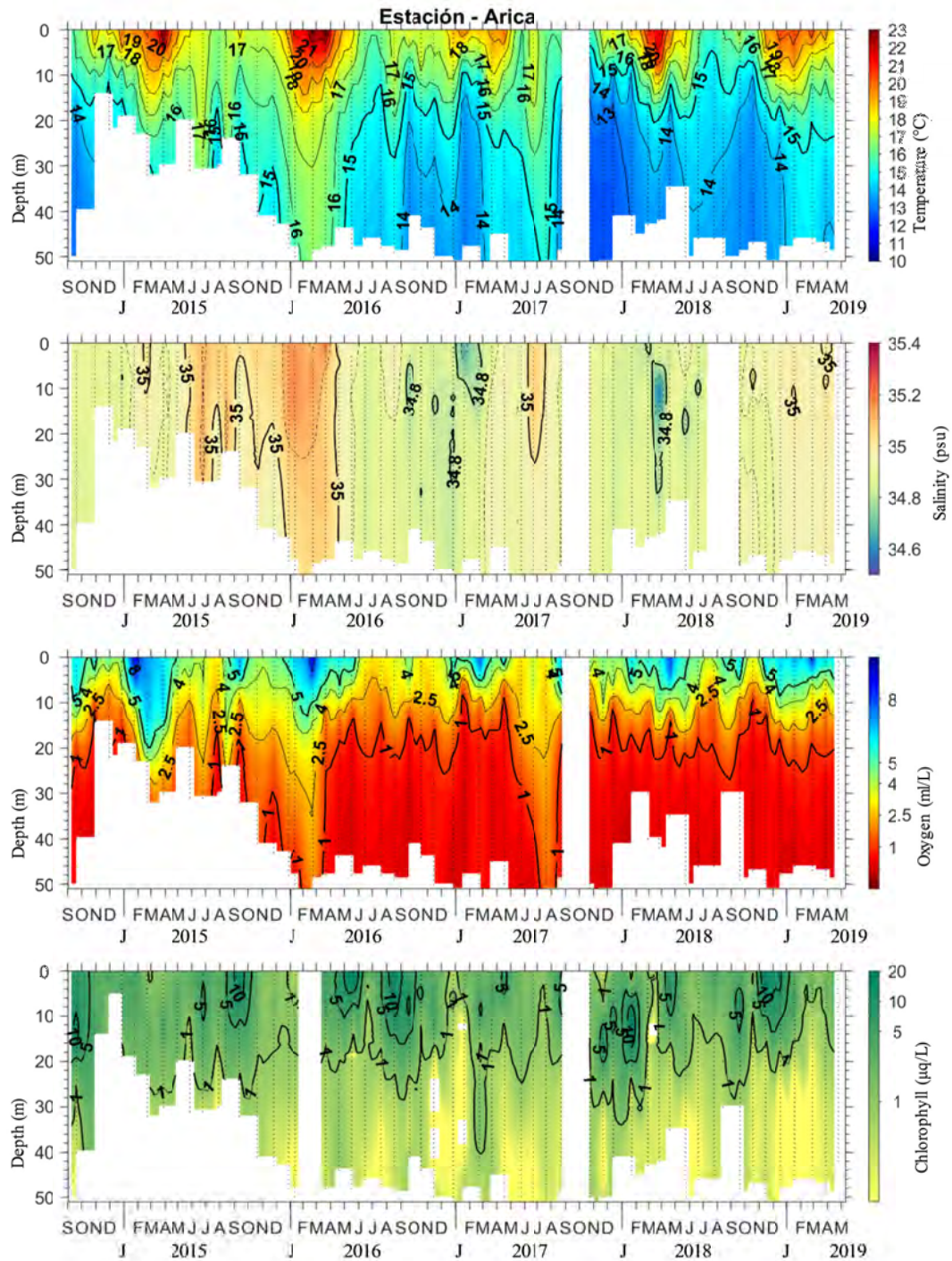




FIGURE 35

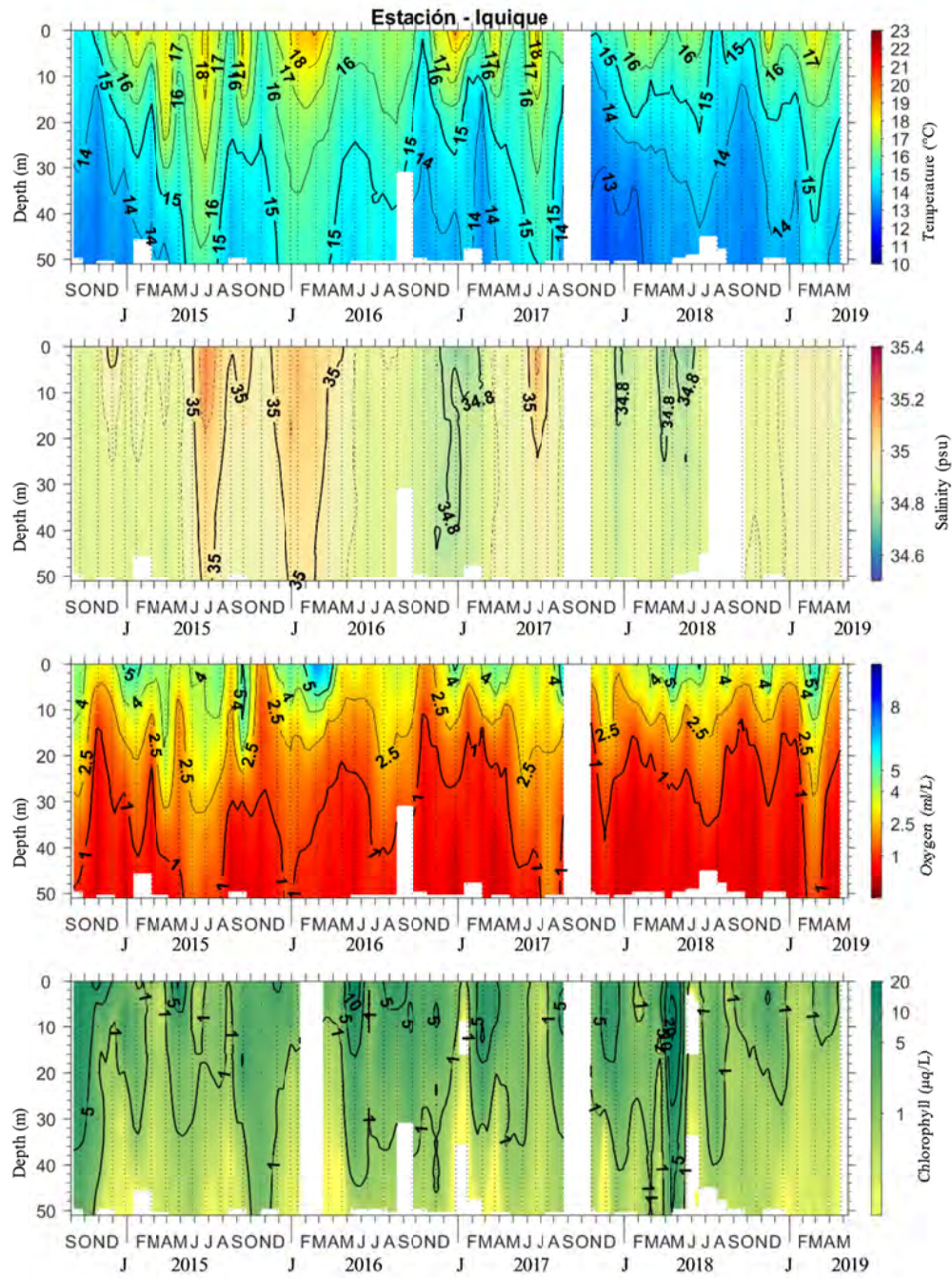






FIGURE 37.

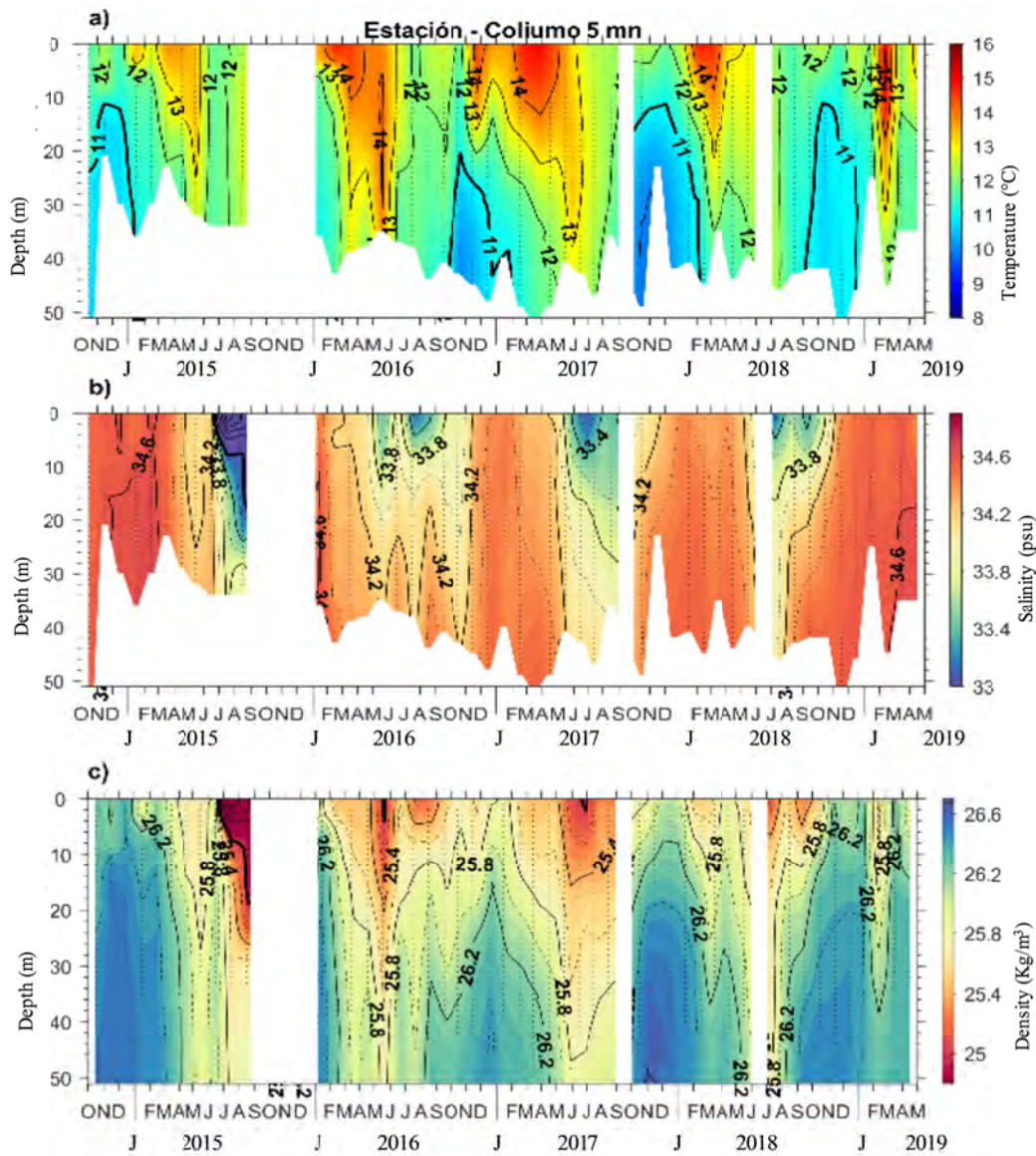




FIGURE 38

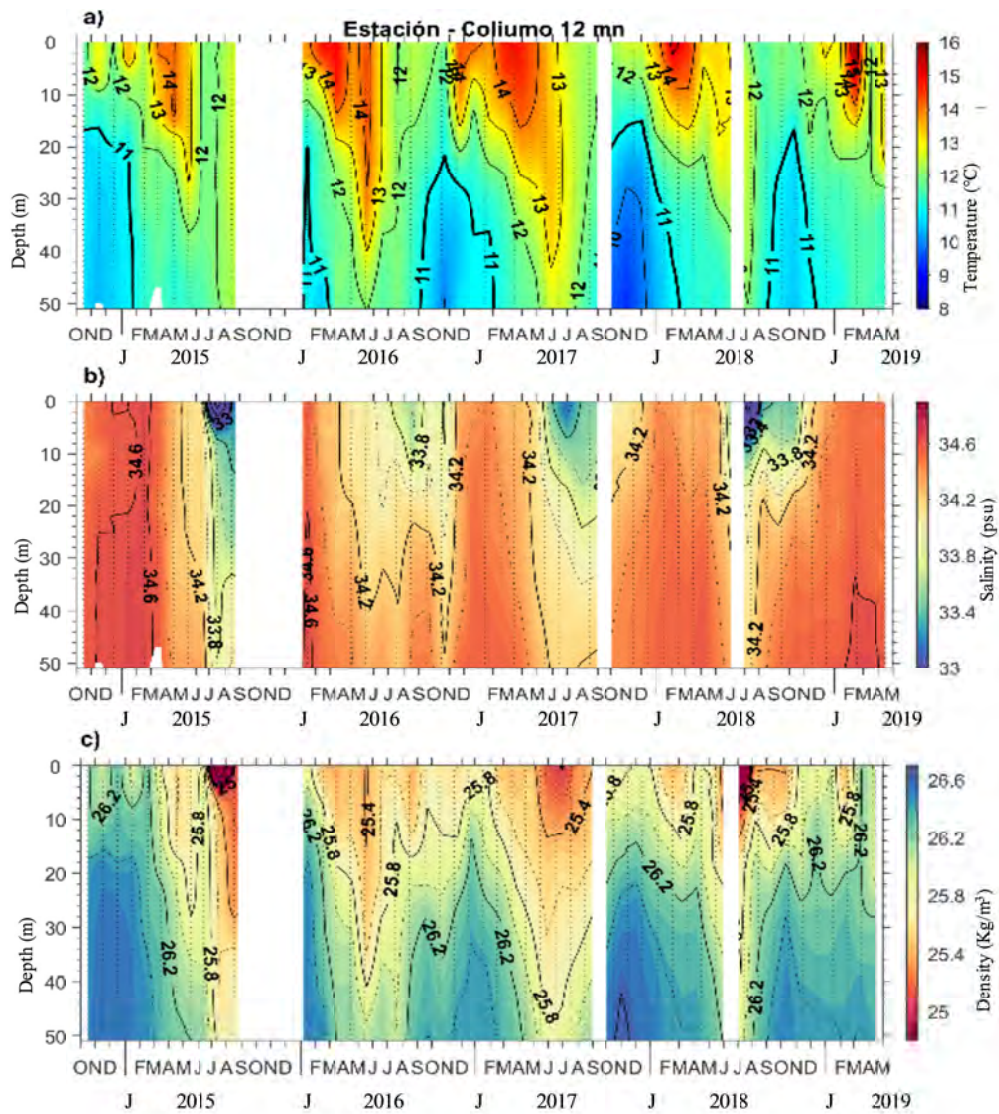


FIGURE 39

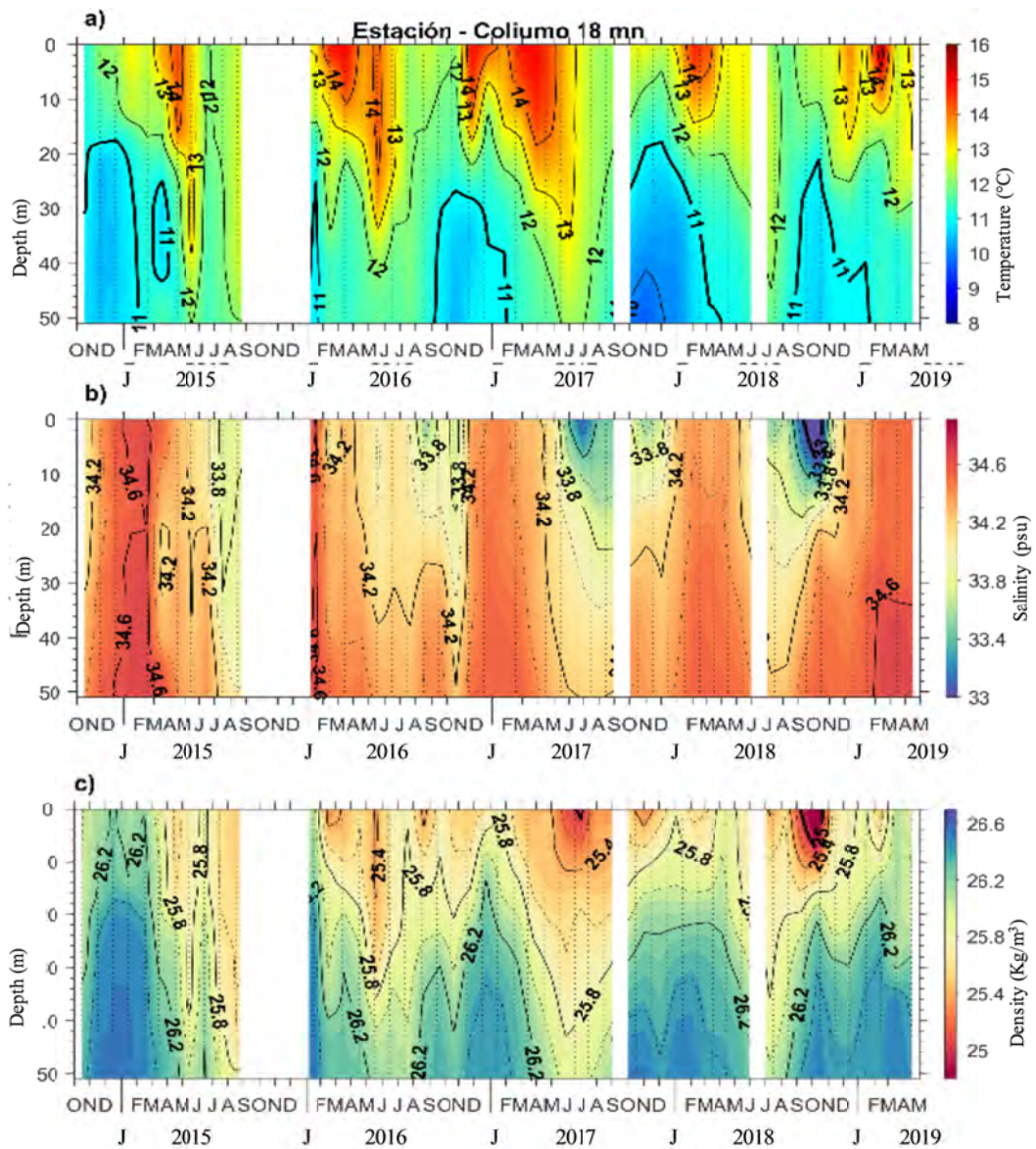




FIGURE 40

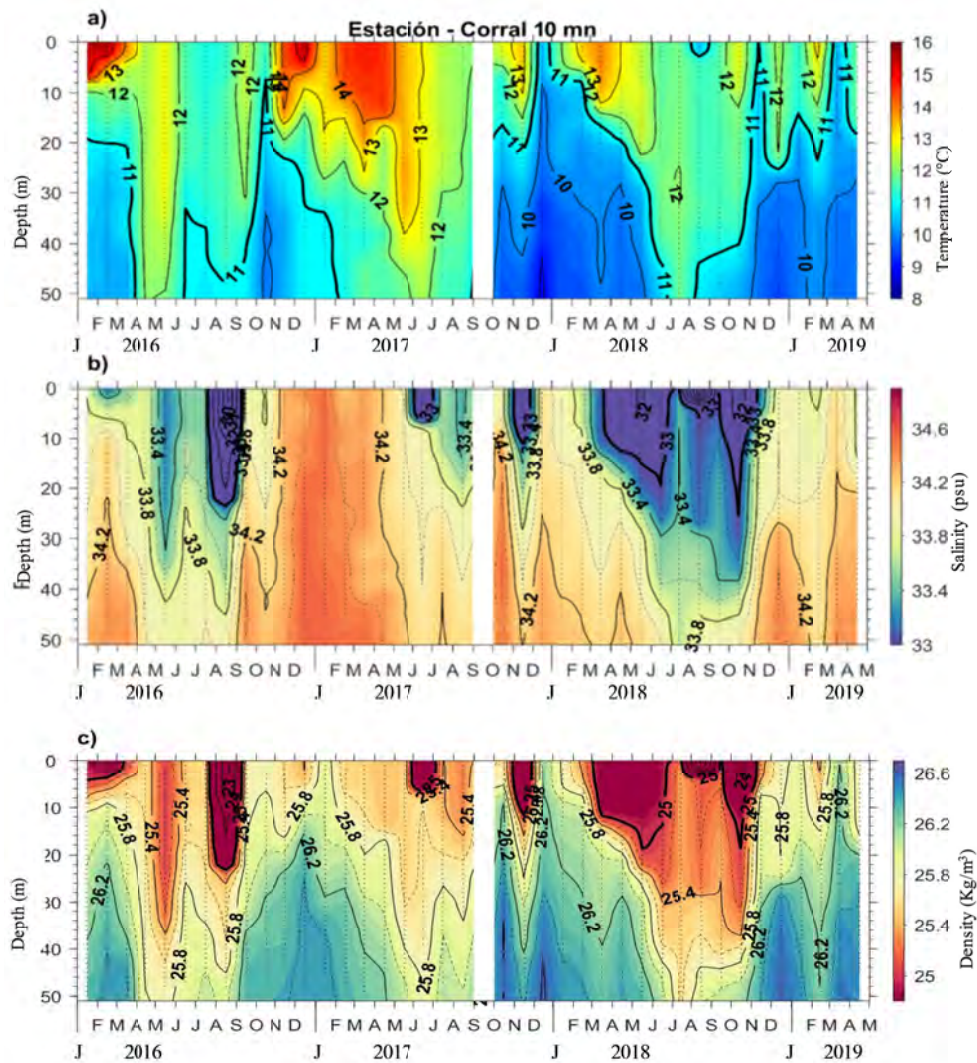


FIGURE 41

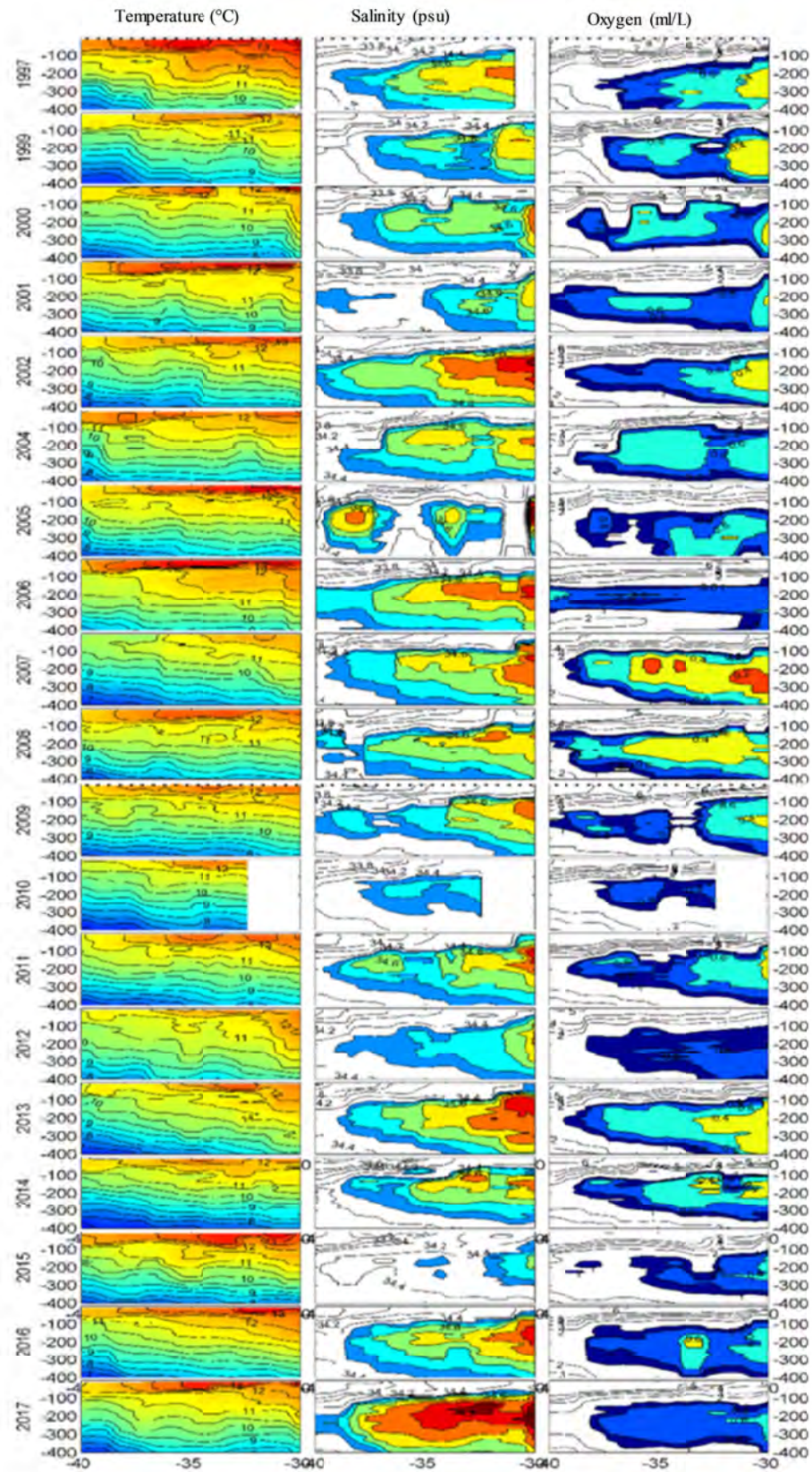




FIGURE 42

